PL-TR-92-2207

THE THEORY BEHIND THE SOCRATES CODE

J. Elgin
L. S. Bernstein

Spectral Sciences, Inc.
99 South Bedford Street, #7
Burlington, MA 01803

6 August 1992

Final Report
9 May 1988 - 8 July 1992

Phillips Laboratory
Directorate of Geophysics
AIR FORCE MATERIEL COMMAND
HANSCOM AIR FORCE BASE, MA 01731-5000

"This technical report has been reviewed and is approved for publication"

Edmond Murad
EDMOND MURAD
Contract Manager

E. Murad
for CHARLES P. PIKE, Chief
Spacecraft Interactions Branch

E. Murad
for CHARLES P. PIKE, Chief
Spacecraft Interactions Branch

This report has been reviewed by the ESD Public Affairs Office (PA) and is releasable to the National Technical Information Service (NTIS)

Qualified requestors may obtain additional copies from the Defense Technical Information Center. All others should apply to the National Technical Information Service.

If your address has changed, or if you wish to be removed from the mailing list, or if the addressee is no longer employed by your organization, please notify GL/IMA, Hanscom AFB, MA, 01731. This will assist us in maintaining a current mailing list.

REPORT DOCUMENTATION PAGE

Form Approved
OMB No. 0704-0188

1. AGENCY USE ONLY (Leave blank)	2. REPORT DATE	3. REPORT TYPE AND DATES COVERED
	6 August 1992	Final Report 09MAY88 - 08JUL92

4. TITLE AND SUBTITLE

The Theory Behind the SOCRATES Code

5. FUNDING NUMBERS

C - F19628-88-C-0074
PE - 62101F
PR - 7601
TA - 30
WU - BB

6. AUTHOR(S)

J. B. Elgin and L. S. Bernstein

7. PERFORMING ORGANIZATION NAME(S) AND ADDRESS(ES)

Spectral Sciences, Inc.
99 South Bedford Street, #7
Burlington, MA 01803-5169

8. PERFORMING ORGANIZATION REPORT NUMBER

SSI-TR-216

9. SPONSORING/MONITORING AGENCY NAME(S) AND ADDRESS(ES)

Phillips Laboratory
Hansom AFB, MA 01731-5000

Contract Manager: Edmond Murad/WSSI

10. SPONSORING/MONITORING AGENCY REPORT NUMBER

PL-TR-92-2207

11. SUPPLEMENTARY NOTES

12a. DISTRIBUTION/AVAILABILITY STATEMENT

Approved for public release; distribution unlimited

12b. DISTRIBUTION CODE

13. ABSTRACT (Maximum 200 words)

The SOCRATES contamination model is described at length. The model allows for unsteady or steady simulation of contamination aboard a spacecraft via the direct simulation Monte Carlo method. The basis for the model is discussed, and sample calculations are given for an RCS engine firing at 320 kilometer altitude for three different orientations. These calculations are compared to visible data in the 6300 Å region which is attributed to the forbidden transition between the $O(^1D)$ and $O(^3P)$ electronic states of atmospheric atomic oxygen.

14. SUBJECT TERMS			15. NUMBER OF PAGES
Contamination Monte Carlo Space Shuttle Rarefied Flows			88
			16. PRICE CODE
17. SECURITY CLASSIFICATION OF REPORT	18. SECURITY CLASSIFICATION OF THIS PAGE	19. SECURITY CLASSIFICATION OF ABSTRACT	20. LIMITATION OF ABSTRACT
UNCLASSIFIED	UNCLASSIFIED	UNCLASSIFIED	SAR

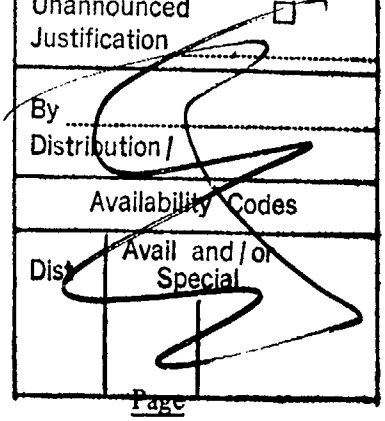

TABLE OF CONTENTS

Section		Page
1.	OVERVIEW OF THE SOCRATES CODE	1
2.	GRID COORDINATES AND GRID STRUCTURE	5
3.	GAS MODEL AND EQUILIBRIUM REFERENCE PROPERTIES	7
	3.1 Preliminary Equilibrium Gas Relations	7
	3.2 Analytical Form of the Collision Cross Section	7
	3.3 Equilibrium Reference Properties for a Multi-Component Gas	10
	3.4 Internal Energy Model	11
4.	INTERNAL REPRESENTATION	13
	4.1 State Vector	13
	4.2 Reduction to a Reasonable Number of Simulated Molecules	13
	4.3 Internal Scales	14
	4.4 Weighting Factors	15
5.	INITIAL AND BOUNDARY CONDITIONS	16
	5.1 Initial Conditions	16
	5.1.1 Number of Simulated Molecules and Their Weighting Factors	16
	5.1.2 Initial Positions	16
	5.1.3 Initial Velocity Components	17
	5.1.4 Initial Internal Energies	18
	5.2 Source Boundary Conditions	18
	5.3 Atmospheric Boundary Conditions	20
	5.3.1 Molecular Flux Across a Surface Element	20
	5.3.2 Incoming Molecular Velocity Components	21
6.	MOLECULAR TRANSLATIONS	22
	6.1 Molecular Translations in Cartesian Coordinates	22
	6.2 Molecular Cloning	22
7.	COLLISION SAMPLING IN A MULTI-COMPONENT VHS GAS	24
	7.1 General Considerations and Approach	24
	7.2 Collision Sampling for a Single Component Gas	24
	7.2.1 Collision Pair Selection	24
	7.2.2 Collision Time Counter for a Single Component Gas	25
	7.3 Collision Class Sampling in Gas Mixtures	26
	7.4 Global Collision Sampling in a Gas Mixture	27
	7.4.1 Global Collision Time Counter	27
	7.4.2 Collision Pair Selection in Multi-Component Mixtures	28

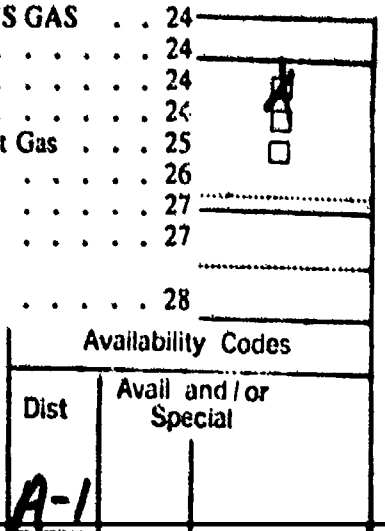

TABLE OF CONTENTS (Continued)

Section		Page
	7.4.3 Summary of Collision Sampling in Multi-Component Mixtures	29
	7.5 Deviations from the General Procedure	30
	7.5.1 Cell Specific Δt_m	30
	7.5.2 Relaxation of Q_{max}	30
	7.5.3 Maximum Time Counter Increment	30
	7.5.4 Separation of Major and Minor Species	31
8.	COLLISION MECHANICS	33
	8.1 Relations for Elastic Collisions	33
	8.2 Effect of Coordinate System	34
	8.3 Simulation of Inelastic Collisions	35
	8.4 Collisions Between Molecules with Distinct Weighting Factors	36
	8.5 Reactive Collisions	37
	8.5.1 Types of Reactive Collisions	37
	8.5.2 Reactive Collision Probability	38
	8.5.3 Options for Simulating Reactive Collisions	38
9.	PROCEDURES FOR COLLISION DOMINATED FLOW	40
	9.1 Collision Cutoff Approach	40
	9.2 Equilibrium Aftermath Approach	40
	9.2.1 Conserved Quantities	41
	9.2.2 Center-of-Mass Velocity Distribution	42
	9.2.3 Molecular Relative Velocity Distribution	43
	9.2.4 Translational Energy of Relative Motion	44
	9.2.5 Determination of Temperature	45
	9.3 The Number of Collisions Required to Achieve Equilibrium	45
	9.4 Method Comparison	46
10.	STATISTICAL SAMPLING OF OUTPUT	47
	10.1 General Considerations	47
	10.2 Sampling of Instantaneous Volumetric Output Quantities	48
	10.3 Sampling of Time Averaged Output Quantities	50
11.	INNER SOLUTION REGION PROCEDURES	51
	11.1 Motivation For The Inner Solution	51
	11.2 General Considerations	51
	11.3 Velocity Variations	52
	11.3.1 Assumed Form of the Velocity Distribution Function	52
	11.3.2 Available Statistics From the Outer Solution	52
	11.3.3 Representation of Available Statistics	53
	11.3.4 Inversion to Determine Equilibrium Procedures	55
	11.3.5 Possible Errors	55

TABLE OF CONTENTS (Continued)

Section		Page
	11.4 Spatial Variations	57
	11.4.1 Reduction to Scaled Variables	57
	11.4.2 Spatial Moments	57
	11.4.3 Analytic Representation of Sampled Moments	58
	11.4.4 Assumed Form for the Flux Distribution	58
	11.4.5 Possible Problems	59
12.	COMPARISON OF SHUTTLE ENGINE FIRINGS IN SPACE TO CODE PREDICTIONS	61
	12.1 Introduction	61
	12.2 Experiment	61
	12.3 Data Reduction	62
	12.4 Modeling Approach	62
	12.5 Results and Conclusions	63
13.	SUMMARY	78
14.	REFERENCES	79

LIST OF ILLUSTRATIONS

Figure		Page
1	A Schematic Representation of the Major Elements of the Shuttle Contamination Problem	2
2	A Diagram of the Basic Solution Procedure Utilized for Steady State Solutions in the SOCRATES Contamination Model	4
3	A Schematic Showing the Basic Design of the SOCRATES Cell Structure Which Uses Cartesian Coordinates with Uneven Spacing	6
4	A Graphical Representation of the Variable r, The Ratio of the Mean Square Velocity to the Square of the Mean Velocity for Molecules from a Maxwellian Velocity Distribution Fluxing Across a Plane, as a Function of the Speed Ratio, w	56
5	A Grayscale Plot Showing the Calculated 6300 Å Plume Radiance for a Ram Burn at 0.4 Seconds	64

LIST OF ILLUSTRATIONS (Continued)

Figure		Page
6	A Grayscale Plot Showing the Calculated 6300 Å Plume Radiance for a Ram Burn at 1.6 Seconds	65
7	A Grayscale Plot Showing the Calculated 6300 Å Plume Radiance for a Ram Burn at 4.0 Seconds	66
8	The Calculated Total 6300 Å Radiant Intensity as a Function of Time for the Three Burn Directions	67
9	A Comparison Between the Calculated and Deduced Peak Total 6300 Å Plume Emission as a Function of Angle of Attack	68
10	The Calculated Contributions of Collisional Excitation and Charge Exchange to $O(^1D)$ Production as a Function of Time for the 180° Angle of Attack Case	71
11	The Calculated Contributions of Collisional Excitation and Charge Exchange to $O(^1D)$ Production as a Function of Time for the 90° Angle of Attack Case	72
12	The Calculated Contributions of Collisional Excitation and Charge Exchange to $O(^1D)$ Production as a Function of Time for the 0° Angle of Attack Case	73
13	The Total Number of Water Molecules in the 0° Solution Region as a Function of Time	74
14	The Contributions of the Three Types of Excitation Collisions Considered as a Function of Time for the 0° Angle of Attack Case	75
15	The Contributions of the Three Types of Excitation Collisions Considered as a Function of Time for the 180° Angle of Attack Case	76
16	The Competing Effects of Collisional Quenching and Radiative Decay as a Function of Time for the 180° Angle of Attack Case	77

LIST OF TABLES

Table		Page
1	Scaling Factors Used for the Internal Representation of Quantities in the SOCRATES Code	14
2	Concentrations of Species Carried in the Model Calculations	63

1. OVERVIEW OF THE SOCRATES CODE

The direct simulation Monte Carlo method, as pioneered by G. A. Bird,[1] provides a powerful technique for the simulation of real gas flows. It bridges the gap between continuum and free molecular flow, retaining validity in either extreme. It can be used to describe complex mixtures, including effects of chemical reactions, heat conduction, viscosity and diffusion for flows in three dimensions. This report describes the application of this technique to the contamination problem, considering flow fields created by the interaction of a spacecraft with the atmosphere. The resultant model has been named the SOCRATES code, which is an acronym for Spacecraft/Orbiter Contamination Representation Accounting for Transiently Emitted Species.

Contamination of instruments on space platforms is an issue of major concern. The shuttle, for instance, gives off matter through surface outgassing, via various thrusters, and from flash evaporators. At altitudes where the atmospheric mean free path is comparable to or less than vehicle dimensions, the deposition back onto instruments will be largely determined by the multiple collision environment surrounding the spacecraft. Even at higher altitudes, this may be the dominant source of contaminants for some portions of the vehicle. In addition to physical contamination of shuttle surfaces, "radiation contamination" is also a potential problem as gases surrounding the spacecraft collide at high speed with atmospheric molecules. These energetic collisions can lead to vibrational, rotational, and electronic excitation and subsequent radiative decay. Ions in the vehicle environment may remain there for some time due to electric field forces, and radiative recombination is another potential source of radiation contamination. The situation is depicted schematically in Figure 1.

Spectral Sciences, Inc. (SSI) has developed this first module of a three-dimensional description of the flow field around a spacecraft so that contamination can be accurately characterized and understood. A comprehensive model of the contaminant field surrounding the space shuttle orbiter, for instance, is crucial to the design of experiments which are to fly on the shuttle and to the development of procedures for minimizing the contamination. The code is designed in a highly modularized fashion so that additional physical and geometric complexity can be added as deemed necessary without requiring major rewriting of the model. The first module of SOCRATES emphasizes the gaseous interactions and their emissions. It is possible to put the results of this code together with a surface model to get a realistic picture of how a vehicle looks in the context of the gaseous emission it produces.

Work has also progressed on adding an inner solution capability to SOCRATES, so that the detailed interaction of the flow field with the vehicle will be accurately described. This work is described in this report, but will be implemented in the second module of SOCRATES.

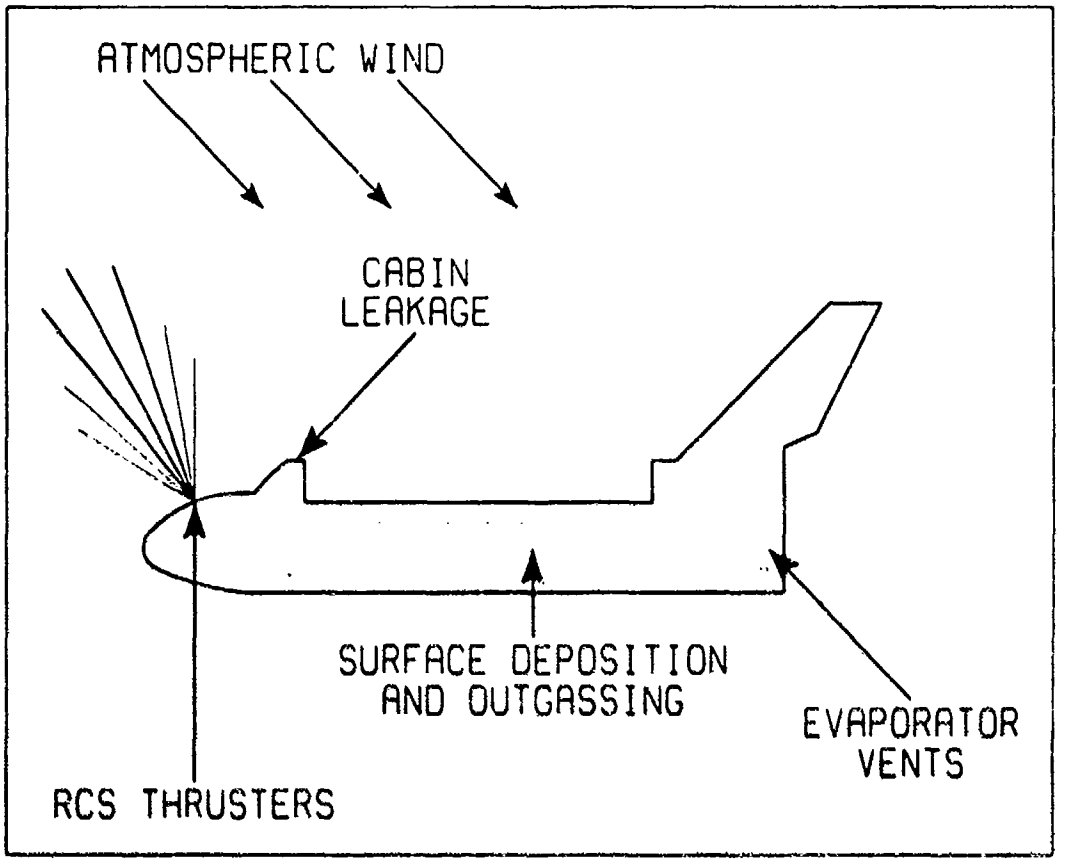

Figure 1. A Schematic Representation of the Major Elements of the Shuttle Contamination Problem.

The basic calculational technique is well described by its originator in Reference 1. However, there have been significant extensions of the method since the publication of Reference 1. The present purpose is to describe how the technique is implemented in SOCRATES; but elementary concepts and relations which are essential to a coherent explanation are included here also.

The direct simulation Monte Carlo method involves storing a discrete number of molecules (via their velocities, positions, and other pertinent information) in a computer. The solution region is broken up into a number of separate cells, and the solution is stepped forward in time in a two stage process. First, the molecules are advanced along their trajectories by an amount appropriate to their velocity and a time increment, Δt_m. In this first stage some molecules will leave the solution region, and some will be introduced as determined by the boundary conditions for a particular problem. The second stage is to simulate collisions in each cell appropriate to Δt_m so that collision frequencies are properly simulated. A basic hypothesis of the method is that if the time step is made small enough, the processes of translations and collisions can be uncoupled in this manner.

Periodically, the solution is sampled by accumulating statistical sums of number densities, velocities and other basic properties. The solution is run repeatedly until statistical deviations are reduced to a desired limit, and then physically meaningful output quantities are computed from the statistical sums. The number of molecules represented is typically many thousand at a time, which is vastly fewer than the number occurring in virtually all real flows. Hence, the construction of a dynamically similar flow to be simulated in the computer is an essential feature of the method.

The logical flow of the solution procedure is shown in Figure 2, which includes the steps described above. The following sections describe in detail the implementation of each of the boxes shown in Figure 2 and the application of the code to some sample problems.

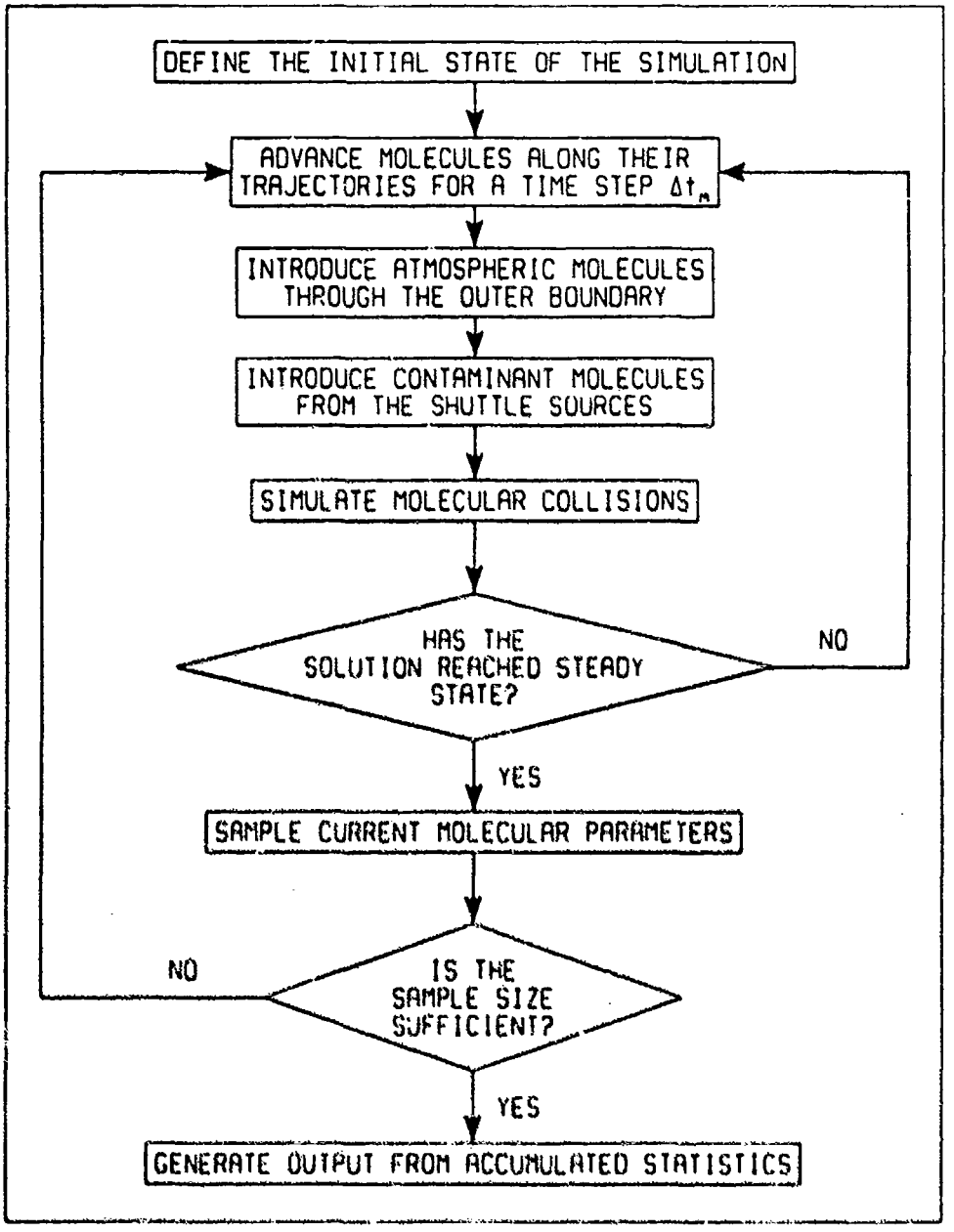

Figure 2. A Diagram of the Basic Solution Procedure Utilized for Steady State Solutions in the SOCRATES Contamination Model.

2. GRID COORDINATES AND GRID STRUCTURE

As discussed in Section 1, the Monte Carlo procedure works by breaking the calculation region up into cells. A solution cell should be a region in which no properties change greatly, i.e., the dimensions of a cell should ideally be small compared to the local scale length of the flow field. Collisions are simulated on a cell-by-cell basis, and molecules can experience collisions only with other molecules in the same cell. There is no other spatial criterion used for determining collision partners, so the cell determines the collision environment for any molecule within it. In addition to defining the collision environment, the other major function of the cell structure is to determine the points at which output is generated. There is no requirement that the cells be divided up in the same coordinate system used in the molecular state vector.

For Monte Carlo calculations, as for other types of computational fluid mechanic analyses, the selection of grid geometry is a critical requirement which is often more of an art than a science. Considerations in the selection of a grid are:

- *The grid should be as simple as possible, since the program must repeatedly decide which cell molecules reside in as they move throughout the solution region.* If this determination required the solution of a complex equation or sifting through tables, the entire program would run significantly slower than if the cell can be determined easily.

- *The grid should concentrate cells where gradients are the largest, so that the least number of total cells (and molecules) are needed to obtain an accurate solution.*

- *The grid should provide flow field information where it is required, with the resolution that is desired for the answer of interest.*

The SOCRATES grid structure is a simple extension of the basic Cartesian coordinate system that is used elsewhere in the code. The cells are determined by the intersection of three families of planes, each family being perpendicular to one of the coordinate directions. For each coordinate, there is a plane at zero and subsequent planes proceed outward in the plus and minus coordinate direction. For instance, the intersection points, x_j, on the positive x axis are given by

$$x_j = x_{max} \frac{\exp(jB/N) - 1}{\exp(B) - 1} \quad , \tag{1}$$

where x_{max} is the position of the last plane (the edge of the solution region in that direction), N is the number of planes intersecting the positive x axis, and B is an adjustable parameter. For B approaching zero, successive planes have equal spatial increments; and as B is increased the planes become more concentrated near the origin. The same relation is applied for planes intersecting the minus x direction, with x_{max} being replaced by x_{min}. The other four directions ($\pm y$ and $\pm z$) are

handled in an analogous fashion. Note that the B and N parameters are specified separately for each of the six directions away from the origin, depending on the physics of the problem under consideration. These values can be input by the user or automatically selected by the program. The SOCRATES grid structure fulfills the objectives enumerated above to a substantial degree. The relations for cell boundary locations are easily inverted to obtain the cell number corresponding to a given position, and the parameter of the distribution allows for concentration of cells in the inner region while allowing larger cells further out where the gradients are less severe.

A sample cell structure resulting from this technique is illustrated in Figure 3. For visual clarity, the number of planes has been limited to two in each of the six directions, since this is the fewest number which illustrates the uneven spacing. A typical calculation would have several times that many planes, but the figure is difficult enough to interpret as it is. A vehicle can be arbitrarily located within this cell structure; though it should be located near the center of the grid structure for it to make sense. Similarly, the wind direction as seen from the shuttle can come from any direction whatsoever; there is nothing in the cell structure or coordinate definition which restricts it.

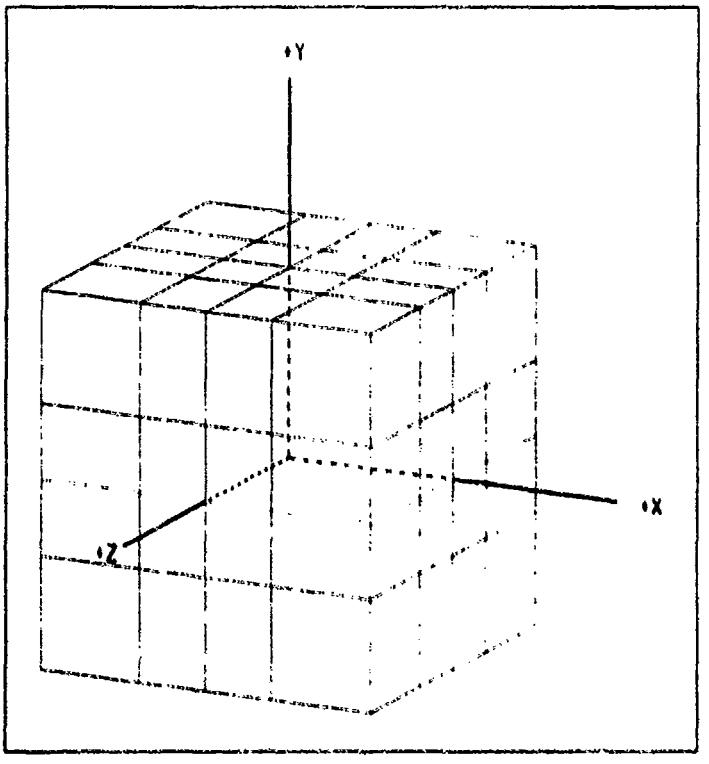

Figure 3. **A Schematic Showing the Basic Design of the SOCRATES Cell Structure Which Uses Cartesian Coordinates with Uneven Spacing.**

3. GAS MODEL AND EQUILIBRIUM REFERENCE PROPERTIES

3.1 Preliminary Equilibrium Gas Relations

The far field equilibrium state has properties which are of relevance to the flow field interaction problem to be solved. In addition to serving to define the proper outer boundary conditions, the far field serves to define length and velocity scales for the problem which are then used to non-dimensionalize the internal code variables. Even if this were not done, it would provide an important comparison case for densities, velocities, collision frequencies, etc.

For a rest gas in equilibrium, the normalized distribution function for the relative speed, c_r, between molecules of species i and molecules of species j is given by[2]

$$f_{ij}(c_r) = (4c_r^2 a_{ij}^{3/2}/\sqrt{\pi}) \exp(-a_{ij}c_r^2) \quad , \tag{2}$$

where

$$a_{ij} = \frac{\mu_{ij}}{2R_0 T_\infty} \quad , \tag{3}$$

and μ_{ij} is the reduced mass of the pair; i.e.,

$$\mu_{ij} = \frac{m_i m_j}{m_i + m_j} \quad , \tag{4}$$

with m_i and m_j representing the masses of the two species. In these relations, T_∞ is the far field temperature and R_0 is the universal gas constant. (R_0 is used instead of Boltzmann's constant since the molecular masses will be consistently represented in atomic mass units rather than grams.) The available translational collisional energy between the two molecules, E_c, is given by

$$E_c = \frac{1}{2}\mu_{ij} c_r^2 \quad . \tag{5}$$

3.2 Analytical Form of the Collision Cross Section

Whenever the direct simulation Monte Carlo method is applied, it is necessary to make trade-offs between accuracy and simplicity in molecular models. It does no good to use a complex molecular potential surface and then find that reasonable computer run times result in very large statistical fluctuations in the output. Since the final output will reflect errors in the statistics as well

as errors in the models, there is a strong impetus to use models which contain the essential physics, but which can be applied in a computationally efficient manner. The current state-of-the-art is the Variable-Hard-Sphere (VHS) model.[3] In this model molecules have a collision cross section which varies as an inverse power of the available collision energy. Hence, if σ_{ij} is the collision cross section for collisions of species i with species j, then σ_{ij} is given by a relation of the form

$$\sigma_{ij} = A_{ij} E_c^{-\omega} \quad , \tag{6}$$

where A_{ij} is a constant coefficient. It follows that the effective diameter for molecules of species i, d_i, is implicitly defined as a function of available collision energy by the relation

$$\sigma_{ii} = \pi d_i^2 = A_{ii} E_c^{-\omega} \quad . \tag{7}$$

A_{ii} can be determined from a reference cross section and velocity via

$$A_{ii} = [\sigma_{ii}(m_i c_r^2/4)^{\omega}]_{ref} \quad . \tag{8}$$

If a reference cross section is given for a reference temperature rather than a reference velocity, then the usual choice for the reference velocity is that velocity which has a collision energy equal to the mean collision energy occurring in collisions at the reference temperature. Mathematically, this is equivalent to

$$(c_r^2)_{ref} = \frac{\langle c_r^3 \sigma_{ij} \rangle}{\langle c_r \sigma_{ij} \rangle} \quad , \tag{9}$$

where the angle brackets indicate averages taken over the distribution function given in Equation (2) evaluated for $m_i = m_j$ and $T_\infty = T_{ref}$. Equation (9) can be simplified to give

$$(c_r^2)_{ref} = \frac{4(2 - \omega) R_0 T_{ref}}{m_i} \quad . \tag{10}$$

For simulations involving a large number of species, reference cross sections are frequently not available for all possible collision pairs. In this case it is possible to specify A_{ii} for self-collisions only, and then use Equation (7) to get a molecular diameter as a function of collision energy. Then, applying the relation

$$\sigma_{ij} = \pi[(d_i + d_j)/2]^2 \quad , \tag{11}$$

the coefficient in Equation (6) for interspecies collisions is given by

$$A_{ij} = [\frac{1}{2}(\sqrt{A_{ii}} + \sqrt{A_{jj}})]^2 \quad . \tag{12}$$

For the internal workings of a Monte Carlo code, it is usually more convenient to express the collision cross section as a function of the relative collision velocity rather than the collision energy. This is simply achieved via the relation

$$\sigma_{ij} = B_{ij} c_r^{-2\omega} \quad , \tag{13}$$

where

$$B_{ij} = A_{ij}(\mu_{ij}/2)^{-\omega} \quad . \tag{14}$$

The parameter ω can be related to η, the exponent of distance in an inverse power intermolecular force law via the relation[3]

$$\omega = \frac{2}{\eta - 1} \quad . \tag{15}$$

Hence, hard sphere molecules (for which η goes to infinity) are represented by ω equal to zero. There is a substantial body of evidence, however, that the effective size of molecules does indeed decrease with increasing collision energy, so a positive value of ω is usually a better choice. ω can be determined from molecular beam data, or from its macroscopic implications. For example, if s is the exponent for the variation of the viscosity coefficient with temperature, then it can be shown[3] that

$$s = \omega + 0.5 \quad , \tag{16}$$

so a measurement of the temperature dependence of the viscosity coefficient serves as an indirect determination of ω.

In order to incorporate the model for internal energy transfer to be discussed in Section 8, it is necessary that ω be assumed the same for all interactions. This represents one of the major restrictions in the current state of modeling.

Although the sizes of molecules are allowed to vary in the VHS model in deciding whether or not a collision is to occur, when a collision does occur the post collision velocity components are computed as if it were a hard sphere collision (see Section 8). This results in a substantial computational simplification and yet retains good agreement with the macroscopic predictions of

the more exact model.[3] (See Reference 1 for a discussion of molecular scattering for general power law potentials.)

3.3 Equilibrium Reference Properties for a Multi-Component Gas

One advantage of the VHS model is that the molecules have a well defined cross section, so it is possible to define a mean free path without putting limitations on the minimum deflection angle that is considered. As is the general case for multi-component gases, however, each component has its own mean free path, and the overall mean free path for the mixture must be defined as a weighted average of the mean free paths of the individual species. The somewhat cumbersome relations required to calculate the overall mean free path are given here. It should be noted that the mean free path is calculated only once for a given problem, so the computational effort required to evaluate it is completely negligible.

An individual molecule of species i will suffer collisions with molecules of species j with a frequency ν_{ij} given by

$$\nu_{ij} = n_{j\infty} < \sigma_{ij} c_r > \quad , \tag{17}$$

where $n_{j\infty}$ is the number density of species j and $< \sigma_{ij} c_r >$ is the average product of cross section times relative velocity for the two species, obtained by integrating over the distribution function given in Equation (2). When this operation is performed, the result is

$$\nu_{ij} = 2B_{ij} n_{j\infty} \Gamma(2 - \omega) a_{ij}^{\omega - 1/2} / \sqrt{\pi} \quad , \tag{18}$$

where Γ denotes the gamma function.

The total collision frequency for an individual molecule of species i, ν_i, is obtained by summing Equation (17) over all species, i.e.,

$$\nu_i = \sum_{j=1}^{p} \nu_{ij} \quad , \tag{19}$$

and the mean free path, λ_i, for molecules of species i is given by

$$\lambda_i = \frac{< c_i >}{\nu_i} = \frac{1}{\nu_i} \sqrt{8 R_0 T_\infty / (\pi m_i)} \quad , \tag{20}$$

where $<c_i>$ is the mean molecular speed for species i molecules. The mean free path for the gas mixture, λ_∞, is then defined as the number density weighted average of the λ_i via

$$\lambda_\infty = \sum_{i=1}^{p} \frac{n_{i\infty}\lambda_i}{n_\infty} \quad , \tag{21}$$

where n_∞ is the total number density:

$$n_\infty = \sum_{i=1}^{p} n_{i\infty} \quad . \tag{22}$$

A useful velocity scale is given by v_s, defined by

$$v_s = \sqrt{2R_0T_\infty/<m>} \quad , \tag{23}$$

where $<m>$ is the reference mean molecular weight, i.e.,

$$<m> = \sum_{i=1}^{p} \frac{n_{i\infty}m_i}{n_\infty} \quad . \tag{24}$$

v_s is the most probable molecular speed for molecules of the mean molecular weight at the reference temperature.

3.4 Internal Energy Model

The current state of modeling for internal energy effects in Monte Carlo flow field simulations is the phenomenological model of Borgnakke and Larsen.[4] In this model, transfer of energy between internal and translational modes is allowed, but it is necessary to assume that each species has a fixed number of internal degrees of freedom, ζ_i. This is equivalent to assuming a constant specific heat, C_{pi}, for each species which can be related to the number of internal degrees of freedom via

$$\zeta_i = 2\frac{C_{pi}m_i}{R_0} - 5 \quad . \tag{25}$$

Alternatively, ζ_i can be related to the ratio of specific heats for species i, γ_i, by the relation

$$\zeta_i = \frac{5 - 3\gamma_i}{\gamma_i - 1} \quad . \tag{26}$$

The interchange of internal and translational energy will be discussed in Section 8, and the selection of initial conditions will be discussed in Section 5.

4. INTERNAL REPRESENTATION

4.1 State Vector

Each simulated molecule in the SOCRATES code is represented by a state vector which comprises all of the information the code has with regard to that particular molecule. The state vector has:

- *Position elements defining the location of the molecule in Cartesian coordinates.*
- *Three velocity elements, giving the corresponding velocity components in the same coordinate system.*
- *A value for the internal energy (usually rotational) of the molecule.* Note that the basic model does not discriminate between internal modes for a particular species. This can be done, if desired, by introducing separate species for the distinct modes.
- *An indicator identifying the molecular species.* This indicator in turn implies all of the properties associated with that species (molecular weight, number of internal degrees of freedom, name, etc.).
- *An indicator giving the computation cell in which the molecule currently resides.* (This could be calculated from its position, but it is needed so often in the calculation that the extra storage location is justified by the increase in efficiency.)
- *A time element, giving the time at which the molecule will strike a solution surface element if it continues on its current trajectory.*

4.2 Reduction to a Reasonable Number of Simulated Molecules

It is clearly impossible to run a computer simulation with anywhere near the same number of molecules that exist in the actual flow problem. The adjustment that is made to make the simulation possible is to artificially increase the cross section, and decrease the number density, by the same large factor. It is the product of number density and cross section which determines the collision frequency for a given molecule, and it is the collision frequency which must be correctly simulated if the correspondence between the real and simulated flows is to be accurate. This is an essential feature of the direct simulation method which has not always been adequately emphasized. It means that the internal scaling factors do not proceed on a strictly dimensional basis. For example, the scaling factor for cross sections is not the square of the scaling factor for lengths.

4.3 Internal Scales

Many problems are more reasonably handled if the internal calculations are carried out with scaled or dimensionless values. This avoids possible problems such as numerical overflow which can cause an execution time error. Such errors can be particularly insidious and difficult to locate in a code whose very essence involves the random combination of numbers.

The output is produced in physically meaningful dimensional form. Hence, the scaling that is discussed here is irrelevant (or nearly so) to the interpretation of code output; it is strictly a matter of the internal representation.

The choices for length and velocity scales are λ_∞ and v_s as defined in Section 3, which are used to non-dimensionalize the position and velocity elements of the state vector. There is no need to provide further non-dimensionalization of mass beyond representing them in atomic mass units, so none is provided. Hence, the scaling factor for energy is just v_s^2, which is used to non-dimensionalize the internal energy element of the state vector.

Number densities are scaled with respect to the far field ambient number density, n_∞, which leaves only the cross section scaling factor to be determined. This factor follows from the condition of flow similarity, which requires that the probability of a molecule suffering a collision in traveling a given path length be accurately simulated. This dimensionless probability can be expressed as the product of a cross section times a number density times a path length (at least for small enough path lengths), and it is required that this product be the same for dimensional and scaled representations. This implies that the product of the scaling factors for these three quantities be unity and, therefore, that the cross section scaling factor be $1/(n_\infty \lambda_\infty)$. The internal scaling factors used in SOCRATES are summarized in Table 1.

Table 1. Scaling Factors Used for the Internal Representation of Quantities in the SOCRATES Code. All Variables are Defined in Section 3.

PROPERTY	SCALING FACTOR
Length	λ_∞
Velocity	v_s
Time	λ_∞ / v_s
Number Density	n_∞
Mass	a.m.u.
Energy	$(\text{a.m.u.})v_s^2$
Cross Section	$1/(n_\infty \lambda_\infty)$

4.4 Weighting Factors

Statistical weighting factors are a crucial element of a successful Monte Carlo simulation, allowing trace species to be described with reasonable accuracy. The weighting factor is the number of "real" molecules that correspond to each "simulated" molecule. A "simulated" molecule corresponds to one molecule's worth of storage (one state vector) allocated in the program, and the weighting factor is its statistical weight. So, for example, the total number density in a cell, n_{cell} can be expressed

$$n_{cell} = \sum_{i=1}^{p} \frac{N_i W_i}{V} \quad , \tag{27}$$

where N_i indicates the number of simulated molecules of species i in the cell, W_i is the weighting factor for that species in that cell, V is the cell volume, and p is the number of species. The product $N_i W_i$ that appears in Equation (27) is termed the number of "real" molecules of species i in the cell. Note that n_{cell} as calculated by Equation (27) is a scaled value; it would have to be multiplied by n_∞, as shown in Table 1, to become a dimensional evaluation of the number density.

The weighting factors used in SOCRATES are dependent on cell and species. Hence, flow fields where a given species is much more dominant in one portion of the solution region than another can be accurately represented.

A critical error that can occur in Monte Carlo codes is to have the number of simulated molecules exceed the dimensioned limit of the code. On the other hand, it is generally desirable to have as many molecules as is feasible to obtain good statistics. Resolution of these conflicting considerations is complicated by lack of a priori knowledge of what the species number densities will be as a function of space and time. The way the resolution is achieved is by a dynamic adjustment of the weighting factors, as required. This keeps the number of simulated molecules more or less constant while allowing the number of real molecules to adjust as the solution evolves. The introduction of weighting factors, with the ability to adjust them as the solution demands, is an important feature of a Monte Carlo simulation which is to be usable by non-experts.

5. INITIAL AND BOUNDARY CONDITIONS

5.1 Initial Conditions

Since the direct simulation Monte Carlo method is inherently an unsteady technique, an initial state must be specified in order to advance the solution. For situations where a steady state result is desired, it is obtained as the long-time solution to an unsteady problem. In this case the initial conditions have no effect on the eventual solution, but they may well have an impact on the speed with which that state is achieved. For steady state solutions, SOCRATES simply starts with an evacuated solution region. For unsteady solutions, however, it is necessary to start with a molecular distribution which is representative of the conditions at the start of the desired simulation. For SOCRATES these conditions correspond to a uniform flow with the translational and internal modes being in equilibrium. The specification of the initial conditions for unsteady runs, therefore, involves determining the state vector elements consistent with this condition for the desired number of molecules.

5.1.1 Number of Simulated Molecules and Their Weighting Factors

The desired number of simulated molecules for each species in each cell, M_c, is an input quantity. (Typically, simulations aim for a total number of molecules per cell in the neighborhood of 20.) Given the initial number density to be simulated for a species, n_i, (which will have been automatically converted to internal dimensions - see Section 4) the weighting factor for species i in a given cell is simply

$$W_i = \frac{Vn_i}{M_c} \quad , \tag{28}$$

where V is the cell volume. If a species is not initially present in a cell, then it is assigned an initial weighting factor of zero. If simulated molecules come into the cell, the weighting factor from their place of origin will be used to initialize the weighting factor in the cell. As the solution proceeds, the weighting factors are automatically adjusted to keep the average number of simulated molecules of each species in each cell approximately equal to M_c. The one exception to this rule is that the code will always try to keep a sufficient number of major species in a cell to guarantee a proper collision environment, and this sometimes requires more than M_c major species molecules.

5.1.2 Initial Positions

The initial molecules assigned to a cell should have an equal probability of being placed in any volume element of the cell. For the hexahedral cells of SOCRATES, this simply involves

selecting each of the position elements at random from the range appropriate to the cell in question. That is, the x position is selected via the equation

$$x = x_{min} + \beta(x_{max} - x_{min}) \quad , \tag{29}$$

where x_{min} and x_{max} are the positions of the x-faces of the cell in question, and β denotes a random variable which has equal probability of lying anywhere in the interval {0,1}. (β will appear often in this report. Each appearance corresponds, of course, to a unique evaluation of the random variable.) The other position elements are selected analogously.

5.1.3 Initial Velocity Components

The thermal velocity components for a molecule in translational equilibrium (neglecting, for the moment, any mean flow contribution) should be selected from a normalized Maxwellian velocity distribution, $f_0(v)$, given by

$$f_0 = \alpha \exp[-(\alpha v)^2]/\sqrt{\pi} \quad , \tag{30}$$

where

$$\alpha = \sqrt{m/(2R_0T_\infty)} \quad , \tag{31}$$

m is the species molecular weight, R_0 is the universal gas constant and T_∞ is the temperature. Equation (31) applies for each of the molecular velocity components and must be sampled three times for each molecule that comprises the initial state of the simulation. A method for directly sampling from this distribution is

$$A_1 = 2\pi\beta \quad , \tag{32}$$

$$A_2 = \frac{1}{\alpha}\sqrt{-\log(\beta)} \quad , \tag{33}$$

$$v = A_2\sin(A_1) \quad . \tag{34}$$

After the thermal velocity components are determined for each molecule, then any mean flow velocity is simply added on. The velocities are then transformed to internal units.

5.1.4 Initial Internal Energies

The only remaining element of the state vector to be specified is the internal energy. Internal energies for a gas in equilibrium are distributed according to the normalized distribution function f_i given by

$$f_i = \frac{\xi^{\zeta/2-1}\exp(-\xi/2)}{2^{\zeta/2}\Gamma(\zeta/2)} \quad , \tag{35}$$

where ζ represents the number of internal degrees of freedom for the species in question, Γ is the gamma function, and ξ is a dimensionless internal energy, i.e.,

$$\xi = \frac{2E_i}{R_0 T_\infty} \quad , \tag{36}$$

where E_i is the internal energy. Equation (35) is a representation of the chi square distribution for ζ degrees of freedom; procedures for sampling from this distribution are given in Reference 5.

5.2 Source Boundary Conditions

The introduction of source molecules into the simulation is a boundary condition which depends on the specific model for the source in question. SOCRATES includes a "core flow" source, which describes the contamination that results from the scattering of the flow from a thruster back onto the shuttle. For this source, it is important to have a description of the main exhaust flow away from a thruster. (This is to be contrasted with a source which describes the direct contamination of surfaces via impact of exhaust gases. Since the thrusters are not pointed directly at shuttle surfaces, it is the small portion of the flow which leaves the thruster at a large angle from the exhaust centerline which is important in this case.)

The plume gases expand upon leaving the exit plane and adopt an essentially radial flow profile over a distance which is on the order of exit plane dimensions. Since this distance is small compared to the length scales of the interaction of the plume with the atmosphere, it is appropriate to replace the nozzle by a point source of exhaust molecules traveling at their thermodynamic limiting speed with an undisturbed number density distribution given by

$$n_e = \frac{B}{r^2} f(\theta) \quad , \tag{37}$$

where B gives the axial number density decay and θ represents the angle from the thrust axis. The r appearing in Equation (37) is the spherical radius, giving the total distance from the source. The

particular form for $f(\theta)$ that is used in SOCRATES is an asymptotic form of that proposed by Brook,[6] namely

$$f(\theta) = \exp\{-\lambda^2[1 - \cos(\theta)]\} \quad , \tag{38}$$

where

$$\lambda^2 = \frac{1}{1 - C_{fr}} \quad , \tag{39}$$

$$C_{fr} = \frac{1}{2}[1+\cos(\theta_n)]\frac{u_e}{u_m}[1+\frac{1}{\gamma M_e^2}] \quad , \tag{40}$$

$$\frac{u_e}{u_m} = [1+\frac{2}{(\gamma - 1)M_e^2}]^{-.5} \tag{41}$$

and

$$B = \frac{1}{2\pi} n_e A_e \lambda^2 \frac{u_e}{u_m} \quad . \tag{42}$$

In the above relations, u_e, M_e, n_e and A_e denote the exit velocity, Mach number, number density and area, respectively; θ_n is the nozzle divergence half angle, and u_m and γ are the thermodynamic limiting speed and the ratio of specific heats.

In a solution time step Δt_m, $n_e u_e A_e \Delta t_m$ real molecules are introduced. Each molecule is assigned an angle θ which is chosen to be consistent with Equation (38) via

$$\theta = \cos^{-1}[1 + C_1 \log(1 - C_2\beta)] \quad , \tag{43}$$

where

$$C_1 = \frac{1}{\lambda^2} \tag{44}$$

and

$$C_2 = 1 - \exp(-2\lambda^2) \quad . \tag{45}$$

An azimuthal angle is selected at random for the molecule, and then the resulting velocity is represented in the basic Cartesian coordinates utilized by SOCRATES. The molecule is then advanced from the source appropriate to a speed of u_{in} and a time increment which is a random fraction of Δt_m. The process is repeated until the proper number of simulated molecules of each exhaust species have been introduced.

5.3 Atmospheric Boundary Condition

The atmospheric boundary condition for SOCRATES is that molecules should be introduced into the solution region from the outer boundaries in such a way as to simulate the undisturbed ambient flow outside of the solution region.

5.3.1 Molecular Flux Across a Surface Element

The relations for molecular flux across an infinitesimal surface element are given in Reference 1. If q is the molecular flux (molecules per unit area per unit time) crossing a given surface element, then q is given by

$$q = \frac{n_\infty}{2\Lambda}\{\exp(-w^2)/\sqrt{\pi} + w[1+\mathrm{erf}(w)]\} \quad , \tag{46}$$

where

$$\Lambda = \sqrt{m/2R_0T_\infty} \quad , \tag{47}$$

and

$$w = \Lambda u_\infty \cos(\theta) \quad . \tag{48}$$

In these relations, n_∞ and T_∞ represent the ambient number density and temperature for the species in question; m represents its molecular weight; u_∞ represents the mean flow velocity; and θ is the angle between the inward surface normal and the mean flow direction. The flux given by Equation (46) is positive for all values of θ, reflecting the distribution of molecular velocities. However, it does become exponentially small for large negative w. (Note that these relations must be applied on a species-by-species basis; each species has a different spread in its velocity distribution by virtue of its different molecular weight.)

The application of Equation (46) to the flat surfaces comprising the SOCRATES outer boundary is direct, since θ does not change along the face. The total number of molecules to introduce for a time step of Δt_m is simply $q\Delta t_m A$, where A is the area of the flat face in question. Since the flux is constant over a flat face, each position on the face is equally likely as a point for

molecular entry. Hence, for a flat face, the starting molecular position can be simply obtained by selecting a point at random on the face.

5.3.2 Incoming Molecular Velocity Components

For each molecule that is introduced, a local orthogonal coordinate system is set up such that one direction is in the direction of the inward surface normal. Velocity components are first determined in terms of this local coordinate system and then transformed to the main code coordinate system. In the local coordinate system, the velocity components parallel to the surface are determined as discussed above for molecules in the initial condition. The inward component of velocity must be selected in proportion to the distribution h(v) given by

$$h(v) = v \exp\{-[\alpha(v - \langle v \rangle)]^2\} \quad , \tag{49}$$

where $\langle v \rangle$ is the component of the mean flow velocity in the inward normal direction and α is as given in Equation (31). It is possible for $\langle v \rangle$ to be negative, but all incoming molecules must have a positive v value by definition. Hence, this distribution is only sampled for positive values of v. The sampling is done via the acceptance-rejection technique.

6. MOLECULAR TRANSLATIONS

As discussed in Section 1, an essential element of the direct simulation Monte Carlo method is the periodic advancement of simulated molecules along their trajectories. Formally, this is accomplished by updating the position and velocity elements of the state vector. The specific procedures for doing this depend on the coordinate system in which the state vector elements are represented.

6.1 Molecular Translations in Cartesian Coordinates

In Cartesian coordinates, the translation is very direct. Let x, y, and z represent the position coordinates and u, v, and w the corresponding velocity coordinates. If initial and final values of the state vector are represented by a 0 and 1 subscript respectively, then the updated state vector elements corresponding to a translation through a time step Δt are given by

$$x_1 = x_0 + u_0\Delta t \quad , \tag{50}$$

$$y_1 = y_0 + v_0\Delta t \quad , \tag{51}$$

$$z_1 = z_0 + w_0\Delta t \quad , \tag{52}$$

$$u_1 = u_0 \quad , \tag{53}$$

$$v_1 = v_0 \tag{54}$$

and

$$w_1 = w_0 \quad . \tag{55}$$

6.2 Molecular Cloning

When a simulated molecule is translated from one cell to another, the weighting factor for that species will generally be different in the new cell. Since it is the number of real molecules rather than the number of simulated molecules which must be preserved when crossing cell boundaries (statistically, at least), it is necessary to correct for the distinct weighting factors (see Subsection 4.4).

If the weighting factor before translation is W_0, then the simulated molecule represents that many real molecules. If the weighting factor in the new cell is W_1, then W_0/W_1 simulated molecules would be required to represent the same number of real molecules in the new cell. If

this ratio were a whole integer, then this could be accomplished by introducing that many "clones" of the simulated molecules in the new cell. That is, W_0/W_1 simulated molecules would be placed in the new cell, all with the same state vector.

When the number W_0/W_1 is not an integer (the usual case, of course), then the cloning must be done on a statistical basis. So, for instance, if W_0/W_1 were equal to 2.7, then 30% of the time two clones would be produced, and 70% of the time three clones would be produced. Note that the ratio may be less than unity, and the molecule may not be introduced into the new cell at all. (In which case the molecule is removed from the simulation.)

Cloning is a necessary evil inherent in a system with spatially varying weighting factors. It enables such a system to maintain the statistically correct flux of mass and momentum across cell boundaries, but it misrepresents the flux of randomized or thermal energy. This can be seen by an extreme case where a very large number of clones is produced when a simulated molecule crosses a cell boundary. The resulting molecules in the new cell have the correct mass and momentum flux, but since they all have precisely the same velocity they have a null relative velocity and, therefore, a zero temperature. If the weighting factors are not too different between adjacent cells, then the errors introduced by this process are acceptably small. However, it does mean that one cannot arbitrarily improve statistics in one portion of the solution region by selectively reducing the weighting factors there. This was a difficulty which was encountered in the early stages of the direct simulation Monte Carlo method while trying to improve statistics along the axis of axisymmetric simulations, since the cell volumes (and, therefore, the sample sizes) tend to be smallest on the axis.

As is also the case for simulated molecules produced via chemical reactions, it is possible for the weighting factors between successive cells to be so different that a prohibitively large number of simulated molecules would be required to produce the same number of real molecules. The codes sense when a disproportionate number of simulated molecules are being produced for a given species and cell and adjust the weighting factor automatically. As the weighting factor is increased, a proportionate fraction of molecules of that species and cell are removed from the simulation in order to keep the number of real molecules properly represented. This process enables the weighting factors to seek their own proper level without a priori knowledge of the solution. (Periodically, the cells are examined to determine if a certain species has been underrepresented in terms of its number of simulated molecules. If this is found to be the case, then the weighting factor is decreased, allowing weighting factors to float downwards as well as upwards. It is the danger of weighting factors being too small, causing an overflow of code dimensions, which is most critical, however.)

7. COLLISION SAMPLING IN A MULTI-COMPONENT VHS GAS

7.1 General Considerations and Approach

The two general considerations in the sampling of collisions are, as usual, accuracy and efficiency of the simulation. As far as accuracy is concerned, it is crucial that the method in which molecules are selected for collisions be proper. The correct collision frequency must be simulated between various species and, in fact, between the different portions of the velocity phase space for the various species. Furthermore, this frequency of simulated collisions must remain correct without any requirements put on the velocity distribution function; it certainly must not be assumed that there is a Maxwellian velocity distribution.

As far as efficiency is concerned, it is highly desirable to use a method of collision sampling involving a computational effort which is proportional to the number of simulated molecules, N, in a cell. Methods which are proportional to a power of N greater than unity can become prohibitively time consuming as the number of molecules is increased - a limit which should be made as accessible as possible for obvious physical reasons.

7.2 Collision Sampling for a Single Component Gas

The simplified situation of a simulation involving only one species is considered here. This problem is significant in part due to all the attention it has received and, as will be seen, it serves as an important reference case. When there is just one species, then there is just one gas kinetic cross section (though it is still, of course, a function of collision energy), just one molecular weight and just one weighting factor for each cell. In short, just one of everything that has a molecular subscript. Hence, in this subsection all such quantities will be presented without subscripts. The most important simplification of having a single species is that there is just one collision class, i.e., only self-collisions of the given species with itself are possible.

7.2.1 Collision Pair Selection

As discussed in Section 1, collisions are sampled on a cell-by-cell basis until the number of collisions simulated is appropriate to the overall solution time step, Δt_m. The only spatial requirement placed on potential collision partners is that they be within the same cell. In particular, it is not required that they be within a molecular diameter of each other. (Note that if all pairs of molecules were inspected to find those that were sufficiently close to each other, this would involve a computational effort in proportion to the square of the number of molecules in the cell.) The rationale for this is that the cells should be small enough so that macroscopic properties can be assumed constant across the cell. When this is the case, then a molecule within the cell can

be considered typical of a molecule which might exist anywhere within the cell, and molecular location can be ignored when selecting potential collision pairs.

Spatial consideration aside, the probability of any two molecules experiencing a collision is proportional to σc_r, the product of their mutual cross section times their relative velocity. This probability is correctly simulated via an application of the acceptance-rejection technique. A maximum value for σc_r, $(\sigma c_r)_{max}$, is stored for each cell. (This value is updated whenever a greater value is encountered.) Pairs of molecules are selected at random from the cell, and σc_r for that pair is calculated. The ratio r, defined by

$$r = \frac{\sigma c_r}{(\sigma c_r)_{max}} \tag{56}$$

is determined. A random variable, β, is then generated, and the pair of molecules is accepted as collision partners if r is greater than β. This produces the proper relative collision probability without regard to the existing velocity distribution function.

7.2.2 Collision Time Counter for a Single Component Gas

The volumetric collision frequency for a single component gas, ν, (collisions per unit volume per unit time), is given by

$$\nu = \frac{1}{2} n^2 < \sigma c_r > \quad , \tag{57}$$

where, as in Section 3, n represents the number density of the species, and $< \sigma c_r >$ is the average product of collision cross section and relative velocity. At first inspection, it would seem from Equation (57) that a correct simulation of collision frequency would require evaluation of $< \sigma c_r >$, which would mean that all pairs of molecules in a cell would have to be considered. Such a procedure involves a computational effort proportional to N^2 and is to be avoided, if possible, in preference to a method which is proportional simply to N. The alternative approach, introduced by Bird,[1] is the time counter approach. For each collision a time counter, t_c, is incremented by an amount which depends on the relative velocity of the collision. Collision sampling continues in a cell until its time counter has been advanced beyond the overall flow simulation time, at which time the code proceeds to the next cell (which has its own time counter). The time counter increment, Δt_c, is given by

$$\Delta t_c = \frac{2}{V n^2 \sigma c_r} \quad , \tag{58}$$

where V is the cell volume and n is the species number density given by

$$n = \frac{NW}{V} \quad , \tag{59}$$

with W being the weighting factor for the species. It should be stressed that Equation (58) applies for each real collision. As is discussed in Subsections 4.4 and 8.4, each simulated collision corresponds to W real collisions, so when a simulated collision occurs the actual applied increment to t_c is W times the value given by Equation (58). A demonstration of the validity of Equation (58) is given in Reference 7.

7.3 Collision Class Sampling in Gas Mixtures

The above procedure for a single species gas can be extended to a multi-component mixture via consideration of distinct collision classes. In this approach, collision classes are defined by the colliding pair identities. Hence, if there are p species in the simulation then there are $p(p+1)/2$ collision classes, which can be identified by the subscripts of the corresponding molecular pair. (The number of classes is not p^2 since the order of molecule specification is not taken to matter in determining a collision class. Hence, the class identified by the subscripts i,j is not distinct from the class identified by the subscripts j,i.)

In collision class sampling each collision class is sampled separately, and the collision sampling in a cell is not complete until all classes have been considered. Each collision class has its own stored value of $(\sigma_{ij}c_r)_{max}$ and its own separate time counter, t_{cij}. It can be shown that the appropriate time counter increment in this case is

$$\Delta t_{cij} = \frac{1 + \delta_{ij}}{n_i n_j V \sigma_{ij} c_r} \quad , \tag{60}$$

where δ_{ij} is the Kronecker delta which is unity for i=j and zero otherwise. As in the previous section, the above increment applies for each real collision. A simulated collision usually corresponds to W_L real collisions, where W_L is the lesser of W_i and W_j (see Subsection 8.4), so when a simulated collision occurs, the applied increment to t_{cij} is W_L times the result of Equation (60).

7.4 Global Collision Sampling in a Gas Mixture

Although the procedure described above is quite reasonable for, say, a two-component mixture, it becomes exceedingly complicated as the number of species increases. For 10 species, for instance, the program must loop over 55 distinct collision classes for each cell, and storage must be allocated for 110 quantities in each cell. As the number of species increases, the storage requirement for the collision sampling constants quickly becomes greater than the storage required for the molecular state vectors! The obvious simplification is to search for a technique where collisions are simulated simultaneously for all collision classes, with each class having its proper relative probability of being selected. The overall collision sampling then continues until a single time counter indicates that sufficient collisions have been sampled in the current time step and cell.

7.4.1 Global Collision Time Counter

If molecular pairs are selected for collisions such that the various collision classes automatically appear with the proper relative frequency (see below), then it is not necessary to consider separate time counters for all the various collision classes. One approach that could then be applied is to keep a collision time counter for just one collision class and increment it when collisions of that class occur. If the various collision classes are being selected according to their correct relative frequency, then simulating the proper frequency for one collision class will ensure, in the long run, that all collision classes are occurring with the correct frequency. A disadvantage with this approach is the necessity of making an arbitrary choice for the collision class which is to have a time counter. Furthermore, there may be no good choice for a reacting flow where the dominant species can vary strongly from place to place. (Clearly, one would not want to select a class of collision that does not occur in a given cell, since the result would be a never-ending sampling of collisions of other classes.)

The preferred approach is to define a global collision time counter, t_g, which is a weighted average of the time counters of all collision classes; i.e.,

$$t_g = \frac{1}{C}\sum_{i=1}^{p}\sum_{j=1}^{i} D_{ij} t_{cij} \quad , \tag{61}$$

where

$$C = \sum_{i=1}^{p}\sum_{j=1}^{i} D_{ij} \quad , \tag{62}$$

and the D_{ij} are non-negative coefficients which can be selected at will. Note that in this formulation every collision class will result in some increment of the global time counter (unless

D_{ij} is zero for that class), so the collision sampling frequency is not dependent on any one collision class.

It remains, of course, to specify the D_{ij}. A very convenient choice is given by

$$D_{ij} = \frac{n_i n_j}{1 + \delta_{ij}} \quad . \tag{63}$$

Firstly, Equation (63) is convenient because it tends to make the collision classes with the higher collision frequencies count more, resulting in good statistics for t_g irrespective of cell location. (Note that D_{ij} is cell dependent since the species number densities are cell dependent.) Secondly, Equation (63) results in a particularly convenient form for t_g. The normalization factor given in Equation (62) can be summed analytically to give

$$t_g = \frac{2}{n^2} \sum_{i=1}^{p} \sum_{j=1}^{i} \frac{n_i n_j}{1 + \delta_{ij}} t_{cij} \quad . \tag{64}$$

Hence, a collision of class ij, which would produce an increment of Δt_{cij} to its own time counter produces an increment Δt_g to t_g given by

$$\Delta t_g = \frac{2 n_i n_j}{n^2 (1 + \delta_{ij})} \Delta t_{cij} \quad , \tag{65}$$

where, again, n is the total number density of all species in the cell. If Equation (60) is substituted into Equation (65), the result is

$$\Delta t_g = \frac{2}{V n^2 \sigma_{ij} c_r} \quad . \tag{66}$$

Equation (66) is extremely significant since it recaptures the precise form of the time counter increment for a single species (Equation (58)), but indicates that it is completely valid for a multi-component mixture so long as the various collision classes are sampled with the proper relative frequency.

7.4.2 Collision Pair Selection in Multi-Component Mixtures

When considering selection of collision pairs, it is crucial to remember the distinction between real and simulated molecules discussed in Subsection 4.4. Given two simulated molecules

selected at random from within the cell, the probability of their having a real collision is proportional to $W_i W_j \sigma_{ij} c_r$. However, real collisions cannot happen individually; they come W_L at a time, where W_L is the lesser of W_i and W_j. Hence, when a collision is decided upon in the program, W_L of them will occur. To compensate for this, potential collision pairs should be accepted for a collision according to the size of Q given by

$$Q = W_U \sigma_{ij} c_r \quad , \tag{67}$$

where W_U is the greater of W_i and W_j. The relative frequency of real ij collisions will then be proportional to the product QW_L (the relative probability of a pair being accepted for a collision times the number of real collisions occurring when the pair is accepted), which is the desired relation. Selection of collision pairs with the correct relative frequency then assures that incrementing the global time counter as discussed above will give a statistically correct sampling of all collision classes simultaneously.

7.4.3 Summary of Collision Sampling in Multi-Component Mixtures

The results of this subsection can be summarized via the following procedure for the sampling of collisions:

- *Each cell has a (current) value of Q_{max}, the largest value of Q which has been encountered so far in the collision sampling process.* Whenever a larger value of Q is encountered, Q_{max} is set equal to that larger value.
- *Each cell has a current value of the global time counter, t_g.*
- *Pairs of simulated molecules are selected at random from all molecules within the cell.*
- *For each pair, Q, (as defined by Equation (67)) is computed.*
- *The ratio of Q to Q_{max} is computed, and a random variable is generated. The pair is accepted for collision if the random variable is less than that ratio.* (If the pair is not accepted, then another random pair is selected. The process continues until a pair is accepted.)
- *For an accepted pair, the collision mechanics are computed as described in Section 8.*
- *The global time counter is incremented by $W_L \Delta t_g$, where Δt_g is given in Equation (66), and W_L is the lesser of the two weighting factors.*
- *The process continues until the global time counter goes beyond the overall flow time.* At that point the collision sampling is commenced in the next cell.
- *When all cells have had collisions simulated, then the code proceeds to the translation portion. (See Sections 1 and 6.)*

7.5 Deviations from the General Procedure

There are some exceptions to the above relations which have been added to SOCRATES in order make it more efficient. These exceptions are described in the following subsections.

7.5.1 Cell Specific Δt_m

Before collisions are simulated in a cell, the mean residence time of molecules in the cell is estimated using the cell dimensions and the molecular velocities. When collisions are simulated in the cell, it is done for an increment of the global time counter that is 20% of this mean residence time (but no less than Δt_m). Collisions are not again simulated in the cell until the overall flow time has caught up to the global time counter for the cell.

The major reason for doing this is to recognize that some cells will tend to have their molecules remain in them much longer than others. Cells which have longer molecular residence times will tend to have molecules which experience more collisions within the cell. When the number of collisions per molecule becomes sufficiently large, it can be assumed that the molecules in the cell equilibrate with each other, and the equilibrium sampling procedures described in Section 9 can be applied. Since these relations are much faster than direct collision sampling, it is highly desirable to apply them whenever they are valid.

For unsteady simulations the cell specific Δt_m is not applied since it might result in a temporal blurring of the solution.

7.5.2 Relaxation of Q_{max}

The current value of Q_{max} in a cell is reduced by a factor of 0.95 if 20 or more potential collision pairs are rejected in a row. The rejection of collision pairs can become the most time consuming part of the simulation, and a large value of Q_{max} exacerbates the problem. This change means that a cell is not permanently penalized for a single event that once occurred in it, but the change in Q_{max} is not so great as to invalidate the pair selection probability. This modification can, under some collision dominated circumstances, result in an order of magnitude increase in computational speed.

7.5.3 Maximum Time Counter Increment

Since Δt_g is inversely proportional to relative velocity (Equation (66)), when a very low velocity collision does occur, it can result in very large increment to the collision time counter, which effectively turns off collisions in the cell for a long time. Although this is statistically proper in the long run, it can result in a substantial statistical fluctuation in the short run. The

codes do not allow a collision time increment to be greater that Δt_m, the overall step that is used in the solution.

The limitation on Δt_g is achieved by decreasing the weighting factor of the collision below the weighting factor of either of the two colliding molecules. The maximum collision weighting factor, $(W_c)_{max}$, is given by

$$(W_c)_{max} = \frac{1}{2}\Delta t_m V n^2 \sigma_{ij} c_r \quad . \tag{68}$$

The weighting factor that is applied to a collision is actually, therefore, the smaller of $\{W_i, W_j, (W_c)_{max}\}$. If W_c represents this value, then a collision counts as W_c events. In order to maintain an overall correct simulation, the Q described in Equation (67) is actually given by the relation

$$Q = \frac{W_U W_L \sigma_{ij} c_r}{W_c} \quad , \tag{69}$$

and the time increment applied to the global time counter is $W_c \Delta t_g$. (The two molecules then have their state vectors updated as a result of the collision with probabilities of W_c/W_i and W_c/W_j respectively.) Most of the time W_c is equal to W_L, and this procedure reduces to that given above; however, the problem of occasional large time increments is eliminated.

7.5.4 Separation of Major and Minor Species

A problem arises when a cell happens to contain a single molecule of one major species and all other molecules in the cell are minor species with weighting factors considerably less than that of the first molecule. (In treating minor species, the ratio of weighting factors may be as much as 1000 or more.) Since a molecule cannot collide with itself, collisions between major species can not occur in such a cell. The result is that the contribution of major species collisions to the overall time counter are unobtainable; and the entire collision time increment has to be made up with collisions between the single major species and one or other of the minor species. (Collisions between minor species were rare since pairs are selected with a probability which is proportional to the greater weighting factor - see above.) The result of this problem is that vastly too many collisions are simulated between the major and minor species. This is both unphysical and numerically inefficient.

The solution to the problem is twofold: 1) Logic is in the collision routines to recognize when this problem occurs; and 2) The global time counter is redefined in such situations. The different time counter is achieved simply choosing a different definition for the D_{ij} coefficients appearing in Equation (61). Rather than taking a weighted average over all collision classes, it is

possible to take a weighted average over just those collision classes which involve a collision between a major and a minor species. If n_i represents the total major species number density and n_j represents the total minor species number density, then D_{ij} is defined for this case to be

$$D_{ij} = n_i n_j \quad , \tag{70}$$

rather than the value given in Equation (63). The implied increment for the global time counter is given by

$$\Delta t_g = \frac{1}{V n_i n_j \sigma_{ij} c_r} \quad . \tag{71}$$

This counter is then only applied for collisions between the species declared to be major and the species declared to be minor, but the increment that is applied is much larger than if the weighting were over all collision classes. Note that collisions between minor species still occur - they just don't affect the collision time counter. It should be stressed that this modification is only applied for the special case of a cell that has a single major species molecule (defined as a weighting factor at least ten times greater than that of the other molecules). The result of this modification is the return of the correct collision frequency to the simulation and the removal of a substantial numerical problem.

8. COLLISION MECHANICS

8.1 Relations for Elastic Collisions

The purpose of this section is to present relations appropriate to the simulation of a collision in the SOCRATES code. (The question of how molecules are selected for collisions, which is crucial to the proper simulation of collision frequency, was taken up in the previous section.) Conservation of momentum implies that the center-of-mass velocity of the collision pair is unchanged by the collision; and conservation of energy then implies that the magnitude of the relative velocity between the collision partners is also unchanged by the collision.[8] Since the collision is treated as a statistical event, all that remains is to select the direction of the post-collision relative velocity vector from the correct distribution. As mentioned in Section 3, collisions in the VHS model are treated as hard sphere collisions when they occur (though they do not occur with the same velocity dependence as do hard sphere collisions). Hence, as far as the collision mechanics is concerned, the model is a hard sphere model. For hard sphere molecules, all directions for the post-collision relative velocity vector are equally likely. This is the chief computational simplicity of the VHS model.

Let the two molecules be identified by subscripts 1 and 2, with m and $\vec{v}$ denoting their masses and velocities. If i and f indicate initial and final states, then the relations for the collision can be summarized via:

$$\vec{v}_{cm} = \frac{m_1\vec{v}_{1i} + m_2\vec{v}_{2i}}{m_1 + m_2} \quad , \tag{72}$$

$$v_r = |\vec{v}_{1i} - \vec{v}_{2i}| \quad , \tag{73}$$

$$\cos(\theta) = 1 - 2\beta \quad , \tag{74}$$

$$\sin(\theta) = \sqrt{1 - \cos^2(\theta)} \quad , \tag{75}$$

$$\phi = 2\pi\beta \quad , \tag{76}$$

$$\vec{v}_{rf} = v_r[\cos(\theta), \sin(\theta)\cos(\phi), \sin(\theta)\sin(\phi)] \quad , \tag{77}$$

$$\vec{v}_{1f} = \vec{v}_{cm} + \frac{m_2 \vec{v}_{rf}}{m_1 + m_2} \quad , \tag{78}$$

and

$$\vec{v}_{2f} = \vec{v}_{cm} - \frac{m_1 \vec{v}_{rf}}{m_1 + m_2} \quad . \tag{79}$$

Where, again, β indicates a random variable which is evenly distributed on the interval zero to one. Each time that β appears a distinct evaluation of the random variable is implied.

8.2 Effect of Coordinate System

Note that the expression for the post-collision relative velocity vector (Equation (77)) is not coordinate system specific. The indicated vector components can apply to any locally orthogonal coordinate system, since the direction implied is random. The convenient coordinate system to use, of course, is the coordinate system used to define the velocity elements of the state vector.

Although Equation (77) is independent of coordinate system, there is a source of error which is dependent on coordinate system. This error arises from a basic premise of the direct simulation Monte Carlo method, namely that position in the cell is ignored when selecting collision partners. If the velocities are expressed in a coordinate system which has spatially varying basis vectors, then differences in position between the two molecules can imply an erroneous difference in velocity.

SOCRATES makes use of the effect of spatially varying basis vectors to solve an otherwise difficult problem. The problem arises due to the presence of concentrated sources of contaminants, such as thrusters and evaporator vents, which are modeled as point sources producing molecules traveling (initially) directly away from the source. Since there is no length scale to a point source, the assumption that properties are constant for the cells in the immediate vicinity of the source must be invalid. This can result in improper collision sampling if special care is not taken.

If the velocities are expressed in Cartesian coordinates, for instance, then two molecules selected from different positions within the cell containing such a point source can have a substantial relative velocity. This relative velocity is illusory, however, since it merely results from the assumption of a point source and the neglect of spatial differences; there should not be collisions based on this relative velocity since the molecules are, in fact, heading away from each other.

A simple resolution to this problem is to express the source velocity elements in spherical polar coordinates. In these coordinates, every molecule leaves the point source with the same

velocity in the direction of the spherical radius vector. Expressed in spherical polar coordinates, the relative velocity disappears. SOCRATES transforms velocity vectors to spherical polar coordinates for cells in the vicinity of point sources (specifically, when the total number density is greater than three times the ambient number density). Collisions are sampled in the transformed coordinates, and then the velocity elements are transformed back to the normal representation after collisions have been sampled for the cell in question.

8.3 Simulation of Inelastic Collisions

SOCRATES uses the Borgnakke and Larsen[4] phenomenological model for transfer of energy between internal and translational modes. In this model, a collision is assumed to be either perfectly elastic or perfectly inelastic, via a user specified probability. A perfectly inelastic collision is achieved by summing the total pre-collision energy (internal energy of both molecules plus the translational energy of their relative motion, Equation (5)), and then assigning post-collision values from the equilibrium distribution for collisions with that total amount of energy, taking into account the number of internal degrees of freedom in the two molecules. Note that this model has the ability to relax from a nonequilibrium to an equilibrium state via an effective collision number. The ability to exchange internal energy in such a manner comprises a significant increase in capability for Monte Carlo codes beyond the previous models where molecules had no internal energy. It is this capability which enables the codes to realistically predict the macroscopic effects of polyatomic gas flow.

Let ζ_1 and ζ_2 be the number of internal degrees of freedom of the two molecules in an inelastic collision, and E_s be the total collision energy defined by

$$E_s = E_{ci} + E_{1i} + E_{2i} \quad , \tag{80}$$

where E_{ci} is the initial translational collision energy defined by Equation (5), and E_{1i} and E_{2i} are the pre-collision internal energies of the two molecules. Using the procedures presented in Reference 5, the somewhat cumbersome expressions given in Reference 4 can be recast in terms of the chi-square distribution. Post-collision values for the respective energies are given by

$$E_{1f} = \frac{X_1 E_s}{X_1 + X_2 + X_3} \quad , \tag{81}$$

$$E_{2f} = \frac{X_2 E_s}{X_1 + X_2 + X_3} \quad , \tag{82}$$

and

$$E_{cf} = \frac{X_3 E_s}{X_1 + X_2 + X_3} \quad , \tag{83}$$

where X_1 is selected from a chi-square distribution with ζ_1 degrees of freedom, X_2 is selected from a chi-square distribution with ζ_2 degrees of freedom, and X_3 is selected from a chi-square distribution with $2(2 - \omega)$ degrees of freedom. (Efficient procedures for sampling from a chi-square distribution are also given in Reference 5.) The post-collision translational energy is then used to determine a new relative velocity between the two molecules. With this new relative velocity, the previous relations for determining the post-collision velocity elements of the molecules apply for inelastic collisions as well as for elastic collisions.

The fact that the translational energy is selected from a distribution with $2(2 - \omega)$ rather than the 3 degrees of freedom that might be expected for translational energy merits some explanation. It is due to the fact that these molecules are not random samples from the gas, but rather special molecules owing to their being the product of a collision. This point can perhaps best be seen by considering microscopic reversibility, where the inverse collision occurs with the same rate in equilibrium. For this reverse process, molecules participating in it are not all equally probable, since those with greater relative velocities are more likely to collide. Hence, the number of degrees of freedom does take on the value three for the special case of ω equal to 1/2, which is precisely the case of collision frequency being independent of relative velocity. Translational energy in collisions behaves as if it has $2(2 - \omega)$ degrees of freedom.

8.4 Collisions Between Molecules with Distinct Weighting Factors

There is an obvious problem when considering a collision between two simulated molecules with distinct weighting factors, since they represent a different number of real molecules. If W_U and W_L represent the weighting factors for the two molecules, with W_U being greater than W_L, then the collision is generally counted as W_L "events". (More precisely, the weighting factor applied to the collision is generally taken to be W_L.) This is accomplished by always assigning post-collision velocity and energy components to the state vector of the molecule with the smaller weighting factor, but only changing the components of the molecule with the greater weighting factor some of the time. The probability that the molecule with the greater weighting factor will have its components changed is simply W_L/W_U. Statistically, this means that for a large number of simulated collisions, each such simulated collision will average out to W_L real collisions for each species, even though their weighting factors differ. It should be noted that this does violate conservation of momentum and energy on an individual collision basis, but these quantities are conserved in the aggregate over a large number of collisions.

In some cases the collision is assigned a weighting factor W_c which is less than either of W_L or W_U. When this is done, the velocity components and internal energies of the two molecules are changed with a probability of W_c/W_L and W_c/W_U, respectively. (See Section 7.)

8.5 Reactive Collisions

Reactive collisions can be simulated directly. The treatment of reactive collisions is similar to that for inelastic collisions, except that a heat of reaction is added to the total energy expressed in Equation (80). Reactive collisions can result in the disappearance of reactant molecules, with the post-collision state being applied to the product molecules.

8.5.1 Types of Reactive Collisions

SOCRATES has a fairly comprehensive chemistry package which is capable of handling a variety of reactive collisions. Generally speaking, a reactive collision is an event which occurs due to collisions with a probability that depends on the velocity (or energy) of the collisions. The following generic types of reactions are treatable:

1. Specific Bimolecular Reactions, i.e., reactions of the form

   $$A + B \rightarrow C + D \quad ,$$

   where A, B, C, and D are particular species. An example of a reaction of this type is

   $$O + H_2O \rightarrow O + H_2O^* \quad .$$

   (In this example, the vibrationally excited state of water, H_2O^*, is treated as a distinct species.)

2. Generic Bimolecular Reactions, i.e., reactions of the form

   $$A + M \rightarrow B + M \quad ,$$

   where A and B are particular species, and M can be any species. An example of a reaction of this type is

   $$H_2O + M \rightarrow H_2O^* + M \quad ,$$

   which is similar to the previous reaction except that now any molecule can serve to excite the water molecule.

3. Dissociation Reactions, i.e., reactions of the form

   $$A + M \rightarrow C + D + M \quad ,$$

   where M is any molecule, and C and D are the fragments of A that result from dissociation. An example of a reaction of this type is

   $$O_2 + M \rightarrow O + O + M \quad .$$

8.5.2 Reactive Collision Probability

The Monte Carlo program simulates all of the above reaction types by calculating a reactive cross section which is a function of the relative collision energy. When a collision occurs, the reaction is simulated with a probability which is proportional to the ratio of the reactive to collision cross section at the relative velocity for the collision.

There are two options for specifying the reactive cross section. The first is to specify an Arrhenius rate constant, k_r, of the form

$$k_r = AT^n \exp(-E_a/R_0T) \quad , \tag{84}$$

where E_a is the activation energy of the reaction and A and n are parameters of the relation. (R_0 is the gas constant and T is temperature.) The unique reactive cross section, σ^*, corresponding to Equation (84) is given by[3]

$$v_r\sigma^* = \frac{\sqrt{\pi}(1 + \delta_{ij})A}{2R_0^n\Gamma(n + 3/2)} \sqrt{1 - E_a/E_c}\,(E_c - E_a)^n \quad , \tag{85}$$

where δ_{ij} is unity for like reactants and zero for unlike reactants, Γ represents the gamma function and E_c is the collision energy given by Equation (5). Note that a rate constant is defined in terms of an equilibrium velocity distribution, so the correspondence between Equations (84) and (85) can be made. There is no requirement, of course, that the reactive cross section given by Equation (85) be used only in equilibrium situations. When this option is used, only the arrhenius parameters A,n and E_a need be specified; the program automatically computes the corresponding reactive cross section.

For some reactions, the form of Equation (85) is too restrictive, and it is then possible to input a table giving the reaction cross section. The form of the table is of the same functional form as Equation (85), namely the product of the relative velocity times the reactive cross section is given as a function of relative collision energy. Although this form is not standard, it is far more convenient for reactions where one of the reactants is generic ("M"), since there is no correspondence between collision velocity and collision energy until the masses of both reactants are specified.

8.5.3 Options for Simulating Reactive Collisions

SOCRATES has distinct options for simulating reactive collisions which are reflective of different anticipated user needs. In all options, the sampling of the reaction rate (if it is being

performed) is done the same way. Whenever a collision occurs between the two reactants, the reactive cross section is calculated, and the reaction is counted with a weighting factor, W_r, given by

$$W_r = W_c \frac{v_r \sigma^*}{v_r \sigma} \quad , \tag{86}$$

where W_c is the collision weighting factor (see the previous section). Hence, even though the reactive cross section may be significantly smaller than the collision cross section, the statistics on the reaction rate are similar. (The statistics for the reaction rate may converge slower due to the velocity dependence of the reaction cross section; but not due to its absolute magnitude.) If two molecules can participate in multiple reactions, statistics are kept for each reaction.

If products are introduced as a result of the reaction, they can be introduced at every simulated reactive collision with a weighting factor of W_r, or introduced with a weighting factor of W_c, but only W_r/W_c of the time. The difference depends on the importance of tracing product species in the simulation. The former approach will result in more computational effort being spent on the product species, but it will give better statistics on them. In either case, reactants are removed from the simulation with a probability of W_r/W_c in any reactive collision.

9. PROCEDURES FOR COLLISION DOMINATED FLOW

One of the major difficulties in the classical Monte Carlo technique is the attainment of equilibrium, where the collision frequency can become prohibitively large for a direct simulation. There are two basic approaches for this problem, and both are utilized in SOCRATES. The equilibrium modeling is only applied if no products are being introduced into the simulation as a result of chemical reactions. When such products are introduced, collisions are always sampled for the full time increment. The two equilibrium approaches are described below.

9.1 Collision Cutoff Approach

This is the usual method of dealing with a collision dominated flow field. In this method, collisions are sampled in a given cell only until enough have been sampled to guarantee equilibrium. Since further collisions only result in the maintaining of equilibrium, they need not be simulated. It is necessary, of course, to estimate the actual collision frequency and keep proper count of the collisions (in particular the excitations) which are not directly simulated in order to obtain the correct collision frequency. Once a cell has had its collisions cut off in this fashion, a flag is set for it. On subsequent calls, the equilibrium aftermath approach (described in the next section) is applied to the cell. (The equilibrium aftermath approach also calculates collision frequencies and switches back to regular collision sampling if it becomes too low.)

9.2 Equilibrium Aftermath Approach

It is possible to avoid sampling collisions altogether if it is known that the cell is in equilibrium. This is done by calculating the total cell energy and momentum, and then selecting post-collision velocities from the appropriate equilibrium distribution. Although the principle is simple, the application is complicated by the fact that molecules in the cell do not all have the same statistical weight. In some ways (e.g., the determination of mean velocity) the statistical weight acts like an effective multiplication of molecular mass - the greater a molecule's statistical weight, the greater its contribution to the mean flow velocity. In other ways (e.g., the assignment of post-collision thermal velocities) the statistical weight does not affect the result - a light molecule should generally have a large thermal velocity irrespective of its statistical weight.

The second difficulty with the formulation of this approach is the necessity for constraining the total energy and momentum to match the pre-collision values. Hence, it is not proper to calculate the initial energy and then simply sample from Maxwellian distributions with the same mean energy, since such a distribution has a finite probability of producing a molecule with any energy - and the net result would be an unacceptable divergence in the cell energy and momentum from the initial values. Both of these problems are avoided in the steps enumerated below.

The method is implemented by calculating the total momentum and energy in the cell and then "peeling off" one molecule at a time from the others. The internal mode energy and energy of relative motion for that molecule (relative motion with respect to the remaining molecules) are selected from equilibrium distributions, except that a scale factor which is proportional to temperature is temporarily left undetermined. The process is repeated sequentially until all energy modes have been assigned values, and then the overall multiplicative constant is chosen to match the known total energy of the system (thus determining the temperature).

Each molecule is then assigned velocity components which are consistent with the known relative velocity between it and the remaining molecules; and then conservation of momentum determines the mean velocity of the remaining molecules. Again, the process is repeated sequentially until all velocities and internal energies have been assigned.

9.2.1 Conserved Quantities

The total energy and center-of-mass velocity are directly computed via the following procedure:

1) The following sums are evaluated, summing over all the simulated molecules in the cell:

$$S_1 = \sum W_i m_i \quad , \tag{87}$$

$$S_2 = \sum W_i m_i u_i \quad , \tag{88}$$

$$S_3 = \sum W_i m_i v_i \quad , \tag{89}$$

$$S_4 = \sum W_i m_i w_i \quad , \tag{90}$$

$$S_5 = \sum W_i m_i (u_i^2 + v_i^2 + w_i^2) \quad , \tag{91}$$

and

$$S_6 = \sum W_i E_{li} \quad . \tag{92}$$

where W_i, m_i and E_{Ii} are the statistical weighting factor, the mass and the internal energy, respectively, of the ith molecule; and u_i, v_i, and w_i are its velocity components.

2) The center of mass velocity components: u^*, v^*, and w^*, are computed via:

$$u^* = S_2/S_1 \quad , \tag{93}$$

$$v^* = S_3/S_1 \tag{94}$$

and

$$w^* = S_4/S_1 \quad . \tag{95}$$

3) The total translational energy of relative motion between the molecules, E_{tm}, can be represented by:

$$E_{tm} = \frac{1}{2}\sum W_i m_i[(u_i - u^*)^2 + (v_i - v^*)^2 + (w_i - w^*)^2] \quad , \tag{96}$$

although it is more easily evaluated by the mathematically equivalent expression

$$E_{tm} = \frac{1}{2}[S_5 - \frac{S_2^2 + S_3^2 + S_4^2}{S_1}] \quad . \tag{97}$$

4) The total cell energy is therefore given by

$$E_{tot} = S_6 + E_{tm} \quad . \tag{98}$$

9.2.2 Center-of-Mass Velocity Distribution

Given that a group of N molecules is in equilibrium, it is possible to determine the form of the distribution function for their mass averaged velocity, taking into account their different statistical weighting factors. This relation is most easily demonstrated by relating the Maxwellian velocity distribution to the normal distribution of statistics and then utilizing a basic statistical theorem.

A variable, r, is distributed according to a normal distribution if its probability density function, f(r), is given by

$$f(r) = \exp(-\frac{r^2}{2\sigma^2})/(\sigma\sqrt{2\pi}) \quad , \tag{99}$$

where σ^2 is the variance of the distribution. (The distribution has been selected with zero mean since the effect of non-zero means does not influence the velocity differences which are the goal of this exercise.) A basic result of statistics is that if r_1 is selected from a normal distribution with variance σ_1^2 and r_2 is selected from a normal distribution with variance σ_2^2, then the variable r_3 defined by

$$r_3 = \alpha r_1 + \beta r_2 \quad , \tag{100}$$

will follow a normal distribution with variance σ_3^2 where

$$\sigma_3^2 = \alpha^2\sigma_1^2 + \beta^2\sigma_2^2 \quad . \tag{101}$$

If it is recognized that a normal distribution is the same as the Maxwellian distribution for a single velocity component, then this result implies the distribution for the center-of-mass velocity components obtained by averaging over N molecules as in Equations (93) - (95). The result is that this mean velocity follows a Maxwellian velocity distribution appropriate to a "super" molecule whose mass, m_s, is given by

$$m_s = \left(\sum_{i=1}^{N} W_i m_i\right)^2 / \left(\sum_{i=1}^{N} W_i^2 m_i\right) \quad . \tag{102}$$

(The temperature of the distribution, of course, is the same as that used to select the constituent molecular velocities.) Although Equation (102) is not intuitively obvious (to these authors, anyway), it does yield some expected limits. If all of the weighting factors are the same, then m_s is the sum of the masses of the individual molecules. However, if one molecule's weighting factor is much larger than the others (resulting in the center-of-mass velocity of the group being essentially equal to that molecule's velocity), then the distribution of center-of-mass velocity is the same as the distribution for that one molecule.

9.2.3 Molecular Relative Velocity Distribution

The relative velocity between an individual simulated molecule (referred to as "molecule j") of mass m_j with respect to the center-of-mass velocity of N other molecules will, therefore, have the same distribution as the relative velocity between that molecule and another molecule of mass

m_s. It is a well known result that this velocity distribution is a Maxwellian distribution appropriate to a molecule with a reduced mass, μ_{js}, given by

$$\mu_{js} = \frac{m m_s}{m+m_s} \quad . \tag{103}$$

Put in terms of the chi-square distribution which is used extensively in the Monte Carlo model, u_{js}^2 (the square of the relative velocity between molecule j and the center-of-mass velocity of the other N molecules), can be expressed

$$u_{js}^2 = \frac{kT}{\mu_{js}} X_{ij} \quad , \tag{104}$$

where X_{ij} is a variable selected from a chi-square distribution for the relevant three translational degrees of freedom. [k is Boltzmann's constant, and T is the (as yet undetermined) temperature.]

9.2.4 Translational Energy of Relative Motion

The total translational energy of the molecules (which can be expressed as in Equations (87) - (96) above, summing over all N+1 molecules) can be algebraically recast in a form which specifically shows the contribution of relative motion between molecule j and the N other molecules. Specifically,

$$E_{N+1} = E_N + \frac{1}{2}\eta_j u_{js}^2 \quad . \tag{105}$$

In Equation (105), E_N is the translational energy which would result if only the N molecules were included in the previous sums, and E_{N+1} is the value obtained with all of the molecules. The factor in the difference, η_j, is the "reduced weighted mass" between molecule j and all of the other molecules, i.e.,

$$\eta_j = \frac{S_1 W_j m_j}{S_1 + W_j m_j} \quad , \tag{106}$$

where S_1 is as defined in Equation (87), applying the sum to the N remaining molecules. It is crucial to note that m_s, as defined in Equation (102), determines the distribution of relative velocities between m_j and the other N molecules; but η_j, as defined above, determines the amount

of energy associated with that relative velocity. Combining Equations (104) and (105) gives the translational energy contribution, E_{tj}, as

$$E_{tj} = (\frac{1}{2}kT)\frac{\eta_j}{\mu_{js}}X_{tj} \quad . \tag{107}$$

Note that this effectively gives a weighting factor associated with the translational energy contribution of molecule j of η_j/μ_{js}.

9.2.5 Determination of Temperature

The internal energy associated with molecule j, E_{ij}, can be represented simply by

$$E_{ij} = (\frac{1}{2}kT)W_jX_{ij} \quad , \tag{108}$$

where X_{ij} is a variable selected from a chi-square distribution with the number of degrees of freedom appropriate to molecule j's internal modes. As discussed above, this process is then repeated sequentially for each molecule in the cell. Note that "N" in the above relations refers to all remaining molecules which have not had their energies determined yet. This means that m_s, for instance, changes with each molecule since it is defined via a sum over these remaining molecules. The last molecule has no translational energy of relative motion associated with it since there are no remaining molecules for it to be moving with respect to. It does, of course, have internal energy.

Summing all of the E_{tj} and E_{ij} and equating them to the known total energy E_{tot} (as given in Equation (98)) then determines the temperature of the system. It is noteworthy that this temperature is not determined just by the total energy of the system, but also by the statistical sampling process. This is consistent with the fact that any temperature could result in the particular observed velocities; although some temperatures are much more likely to produce them than others.

Once the temperature is defined, then the sequential relative velocities squared u_{js}^2 (Equation (104)) and internal energies (Equation (108)) are determined. It is then a simple matter to go back and apply these values to select individual molecular velocity components via the same procedure described in Section 8.

9.3 The Number of Collisions Required to Achieve Equilibrium

The number of collisions required to achieve equilibrium depends on the model being employed and the criterion for equilibrium. (Equilibrium is approached asymptotically and, as

such, could be regarded as an ideal limit which is never realized.) The model being employed, as discussed in Subsections 3.4 and 8.3 is that of Reference 4. In this "statistical collision" model, a fraction, α, of the collisions are taken to be "perfectly inelastic"; that is, in such collisions all translational and rotational energy of the colliding molecules is made available for distribution to the post-collision state vectors, taking into account the number of translational and internal degrees of freedom. The rest of the collisions are taken to be completely elastic, with no interchange taking place between the translational and rotational energy modes. The parameter of the model, α, should be chosen to match available data for rotational relaxation.

Within the context of this model, the question to be addressed is how many collisions are required in a cell before the model predicts that it is essentially in equilibrium. The question can be made independent of α if it is phrased: "How many inelastic collisions per molecule must be simulated before the cell can be considered to be in equilibrium?". This question is suitable for direct investigation with the model, and a test calculation was performed to answer it. The test calculation indicated that the equilibration is 90% complete after approximately 3.08 inelastic collisions (on the average) for each molecule. This seems to represent a reasonable point at which to say that further collision simulation is unnecessary, although the cutoff is of necessity somewhat arbitrary. This number of inelastic collisions serves as a useful benchmark in the comparison of the collision cutoff and equilibrium aftermath approaches, and it also serves to define when the application of the equilibrium aftermath approach is valid.

9.4 Method Comparison

Test runs were run where the collision cutoff approach was utilized for 3.08 inelastic collisions per molecule. (Since $\alpha = 0.2$ was used, this corresponded to about 15 total collisions per molecule.) The time required to compute the relaxation via collisions was then compared to the time required to utilize the equilibrium aftermath approach. The result was that the equilibrium aftermath approach was almost an order of magnitude (a factor of 9) faster in achieving the same result. This ratio will no doubt vary with computer and specific calculation being performed; but it is highly likely that the equilibrium aftermath will always come out considerably faster. It is for this reason that the method was implemented in SOCRATES.

10. STATISTICAL SAMPLING OF OUTPUT

10.1 General Considerations

It is safe to say that the molecular state vectors as they exist in the computer do not comprise the usual desired output of the procedure. With rare exceptions, it is the macroscopic quantities such as temperature, density, mean flow velocity, etc. which are of interest - not the microscopic quantities represented by the state vector of an individual simulated molecule. The generation of the desired output requires that the macroscopic quantities of interest be represented in terms of statistical sums of the available microscopic quantities; and it is the main purpose of this section to present these correspondences. All sums are kept in terms of "real" molecules and events, i.e., the current weighting factors are included in the sums. This is essential since the weighting factor determines the statistical importance of a given molecule. Since the weighting factors are dynamically and unpredictably adjusted as the solution progresses, it would not be possible to go back and add in the effect of weighting factors a posteriori.

In general, it must be decided ahead of time exactly what output is desired from the code, and, therefore, what statistical sums should be kept to generate it. There is a vast amount of potential information in the simulation, and it is not reasonable to store all possibly interesting quantities in all runs. On the other hand, it is wasteful to completely rerun a case just because the user decides there was an additional quantity he was interested in. The selection of output for a given run, therefore, unavoidably requires user judgment. Once the user has decided upon the required output, the determination of which statistical sums are required is done automatically by the code. Care is taken to make sure that a statistical sum is not duplicated internally if it is required by more than one requested output quantity.

Some initial words of caution are required. By its nature, the direct simulation Monte Carlo method works with far fewer molecules than nature does and it, therefore, exhibits considerably greater statistical variation in its macroscopic predictions. To reduce these variations, the code is run repeatedly for the same case, increasing the statistical base from which the macroscopic output is derived. Useful results can usually be obtained with a modest computational effort. However, this statement must be tempered by a realization of the convergence rate for Monte Carlo sampling. Basically, the statistical error in the output converges as one over the square root of the sample size (or run time). Hence, if a solution looks good, but the user decides he would like one more significant digit (i.e., he would like the statistical error to be reduced to 0.1 times its current value) it would require that the run time be increased by a factor of 100! It can be seen that the desire for more accuracy can quickly turn the most efficient code into a money gobbling nightmare. When using a Monte Carlo technique, one must accept some statistical scatter in the output.

10.2 Sampling of Instantaneous Volumetric Output Quantities

Instantaneous volumetric output quantities, such as density, temperature and velocity, can be determined by examining the molecular state vectors at a particular time in the simulation. The code pauses in the simulation and uses the molecular state vector elements to add values to the statistical sums appropriate to the various cells and the particular time that it paused. It then proceeds with the simulation until the next sampling time. As the code goes through its successive runs, it stops at the same points in the simulation every time and adds to the statistical base for the sums. (For steady state cases, it simply does it repeatedly after the initial transient has died down.) The items listed below, with their statistical definitions, are selectable as output requests in SOCRATES. Summations are performed over all applicable simulated molecules, which include N_{run} separate runs.

- TOTAL NUMBER DENSITY

$$n = \frac{S_1}{VN_{run}} \tag{109}$$

- MEAN MOLECULAR WEIGHT

$$m = \frac{S_6}{S_1} \tag{110}$$

- x VELOCITY COMPONENT

$$v_x = \frac{S_3}{S_6} \tag{111}$$

- y VELOCITY COMPONENT

$$v_y = \frac{S_4}{S_6} \tag{112}$$

- z VELOCITY COMPONENT

$$v_z = \frac{S_5}{S_6} \tag{113}$$

- OVERALL TRANSLATIONAL TEMPERATURE

$$T = \frac{1}{3R_0S_1}\left(S_2 - \frac{S_3^2 + S_4^2 + S_5^2}{S_6}\right) \tag{114}$$

- TRANSLATIONAL TEMPERATURE IN jTH DIRECTION

$$T_j = \frac{1}{R_0S_1}\left(S_7 - \frac{S_8^2}{S_6}\right) \tag{115}$$

- INTERNAL MODE TEMPERATURE

$$T_I = \frac{2S_9}{R_0S_{10}} \tag{116}$$

where the indicated sums, S_k, are defined by:

$$S_1 = \sum_i W_i \ , \tag{117}$$

$$S_2 = \sum_i W_i m_i (v_{1i}^2 + v_{2i}^2 + v_{3i}^2) \ , \tag{118}$$

$$S_3 = \sum_i W_i m_i v_{xi} \ , \tag{119}$$

$$S_4 = \sum_i W_i m_i v_{yi} \ , \tag{120}$$

$$S_5 = \sum_i W_i m_i v_{zi} \ , \tag{121}$$

$$S_6 = \sum_i W_i m_i \ , \tag{122}$$

$$S_7 = \sum_i W_i m_i v_{ji}^2 \ , \tag{123}$$

$$S_8 = \sum_i W_i m_i v_{ji} \ , \tag{124}$$

$$S_9 = \sum_i W_i E_{Ii} \tag{125}$$

and

$$S_{10} = \sum_i W_i \zeta_i \quad . \tag{126}$$

With the exception of Equation (110), all of the above quantities can also be defined and calculated for any specified species. The sums are the same except that only molecules of that species are considered. Before printing output quantities, they are always transformed to standard dimensions from the internal dimensionless variables.

10.3 Sampling of Time Averaged Output Quantities

Some additional quantities of interest are not sampled at a separate sampling time as described above, but rather as the simulation evolves. Examples of such quantities are collision rates, reaction rates, mean velocities between molecules, etc. For the most part, these quantities depend on the relative state of more than one type of molecule, and they are by their nature expressed as average values over a finite time interval. The formulas for calculating these quantities are no more than event counters, and will not be included here. The following quantities are currently available as output:

- Mean Relative Velocity Between any Two Species;
- R.M.S. Deviation of Mean Relative Velocity Between any Two Species;
- Mean Product of Cross Section Times Relative Velocity Between any Two Species;
- Collision Rate Between any Two Species;
- Reaction Rate for any Chemical Reaction;
- Reaction Rate for any Photochemical Reaction;
- Flux Rate for any Species on any Surface Element.

The sampling for all but the last of these quantities occurs in the collision simulation routines. As pairs are considered as possible collision partners, statistics are kept to generate the first three quantities. Statistics on collisions and reactions are kept as they occur, and the last quantity is determined in the molecule advancement routines.

11. INNER SOLUTION REGION PROCEDURES

11.1 Motivation For The Inner Solution

The separation into an inner and outer solution is necessitated by the physical and computational realities of the interaction between contaminant molecules and the surrounding atmosphere. The problem is created by the combination of the following two points: 1) In order to describe the scattering of contaminant molecules, the solution region must extend several mean free paths from the source of the contamination, which typically means tens of kilometers; and 2) At the same time, in order to describe the detailed interaction between the flow field and the specific geometry of the vehicle in question, cells must be smaller than characteristic length scales of the vehicle. Combining these two requirements in a three dimensional flow situation means that many more cells and simulated molecules are required than is computationally feasible. However, the two requirements naturally lend themselves to two distinct solutions, which are referred to as the "inner" and "outer" solutions. The outer solution determines the scattering of the contaminants by the atmosphere and doesn't require solution cells which are small compared to the vehicle, since the characteristic length scale for this scattering is much larger than the vehicle. Hence, the outer or scattering solution can be carried out first, with all contaminant sources assumed to be merely at the origin. The outer solution then determines the rate at which both scattered and atmospheric molecules will be approaching the vicinity of the vehicle, and this (rather than the undisturbed free stream) can then be used as a boundary condition for the inner solution, allowing its outer boundaries to extend to just beyond the vehicle.

11.2 General Considerations

The boundary conditions for solutions via the Direct Simulation Monte Carlo method involve introducing molecules at the boundaries which have statistically correct fluxes, velocity distributions, and internal energies. Only the inwardly directed portion of the velocity distribution function is relevant; the outward portion follows naturally from the solution.

For a general nonequilibrium flow, it can be a formidable task to determine the complete inward velocity distribution at the boundaries so that molecules may be introduced properly. Generally, therefore, the boundaries are merely placed far enough away from the interaction region so that the flow may be assumed to be in equilibrium at the boundaries. Since an equilibrium flow has a velocity distribution which is characterized by the well known Maxwell-Boltzmann function, it is then straightforward to determine a statistically correct procedure for molecule introduction.

Such a procedure is clearly not adequate for the inner solution described above. The ambient flow is likely to be disturbed near the vehicle where the inner solution boundary is to be placed, and the flux of scattered contaminants back into the solution region would be completely lost if the normal boundary condition were used. The procedure that is used, therefore, is to gather

relevant statistics in the outer solution, and devise a boundary condition for the inner solution which is consistent with these statistics.

11.3 Velocity Variations

11.3.1 Assumed Form of the Velocity Distribution Function

The procedure that is being adopted is to use a generalized form of the equilibrium distribution function. The generalizations that are applied are as follows: 1) Each species is allowed to have its own mean flow velocity. (In equilibrium, all species would have the same mean velocity.) 2) Each species is allowed to have its own translational temperature, and this temperature is allowed to be distinct for the three coordinate directions. (In equilibrium, all species would have the same temperature, and it would not vary with coordinate direction.) 3) Each species is allowed its own internal mode temperature. (In equilibrium, this temperature would be the same for all species, equal to the common translational temperature.) Quantitatively, it is assumed that for the ith species, the velocity distribution in the jth direction follows the functional form:

$$f_{ij}(u_{ij}) = (\alpha_{ij}/\sqrt{\pi})\exp[-\alpha_{ij}^2(u_{ij}-\overline{u}_{ij})^2] \tag{127}$$

where

$$\alpha_{ij} = \sqrt{m_i/(2R_0T_{ij})} \quad . \tag{128}$$

In these relations, m_i is the molecular weight of the ith species in atomic mass units, R_0 is the universal gas constant, and T_{ij} and $\overline{u}_{ij}$ represent the translational temperature and mean velocity, respectively, of the ith species in the jth direction. By definition of f_{ij}, the probability of a molecule of species i having a velocity component in the jth direction between u_{ij} and $u_{ij}+\Delta u_{ij}$ is $f_{ij}(u_{ij})\Delta u_{ij}$. Under this assumption, therefore, the equilibrium boundary condition can be applied for each species (including those not present in the free stream) by determining the parameters $\overline{u}_{ij}$ and T_{ij}, as well as the effective density of the species, n_i.

11.3.2 Available Statistics From the Outer Solution

The outer solution will have the location of the outer boundary of the inner solution specified. This boundary will be subdivided into rectangular elements which may (but need not necessarily) be particular cell boundaries for the outer solution. For each rectangular element, whenever a molecule crosses that boundary in the outer solution, moving into the inner solution region, statistics can be kept. In addition to just counting the molecules of each species, it is also

possible to keep velocity and spatial moments of the flux of each species. This section will demonstrate how velocity moments can be used to determine the parameters $\overline{u}_{ij}$ and T_{ij}, as well as the effective number density n_i, appropriate to a particular rectangular element. Subsection 11.4 will deal with spatial variations along the rectangular element.

Let $\overline{i}_1$ be the inward normal at the surface element and $\overline{i}_2$ and $\overline{i}_3$ represent two other unit vectors such that $\overline{i}_1$, $\overline{i}_2$ and $\overline{i}_3$ form an orthonormal triple of unit vectors. Depending on the orientation of the rectangular element, each of these unit vectors will be either aligned or anti-aligned with one of the three basic solution unit vectors: $\overline{i}_x$, $\overline{i}_y$ and $\overline{i}_z$. Keeping statistics in the $\overline{i}_2$ and $\overline{i}_3$ directions is straightforward, following the procedures described in the previous section. The more difficult task is to determine the effective equilibrium gas quantities for the direction aligned with the normal of the surface element, $\overline{i}_1$. As molecules cross the boundary segment, the following statistics (among others) can be kept for each species:

a) $\dot{q}_i$; The flux of species i in molecules/(cm^{2}s).

b) $<u_{i1}>$; The mean value of the 1st velocity component.

c) $<u_{i1}^2>$; The mean square value of the 1st velocity component.

Note that the sampling is applied only for molecules which cross the boundary with a positive velocity component in the $\overline{i}_1$ direction, so that all molecules included in these statistics will by definition have a positive value of u_{i1}. Since only molecules with a positive u_{i1} component are included in the statistics, and since the molecules with large u_{i1} components will tend to flux across the boundary faster and be counted with a larger weight, ***it is not the case that*** $<u_{i1}>$ ***is equal to*** $\overline{u}_{i1}$.

11.3.3 Representation of Available Statistics

For a Maxwellian velocity distribution (Equation (127)), it is possible to directly compute the expected values of the available statistics. The results are:

$$\dot{q}_i = n_i \int_0^\infty u_{i1} f_{i1}(u_{i1}) du_{i1} \quad , \tag{129}$$

$$<u_{i1}> = \frac{n_i}{\dot{q}_i} \int_0^\infty u_{i1}^2 f_{i1}(u_{i1}) du_{i1} \tag{130}$$

and

$$\langle u_{i1}^2 \rangle = \frac{n_i}{\dot{q}_i} \int_0^\infty u_{i1}^3 f_{i1}(u_{i1}) du_{i1} \quad . \tag{131}$$

Substituting the expression for f_{i1} given in Equation (127), and performing a little algebra, these expressions can be written:

$$\dot{q}_i = \frac{n_i I_1(-w)}{\alpha_{i1}\sqrt{\pi}} \quad , \tag{132}$$

$$\langle u_{i1} \rangle = \frac{I_2(-w)}{\alpha_{i1} I_1(-w)} \tag{133}$$

and

$$\langle u_{i1}^2 \rangle = \frac{I_3(-w)}{\alpha_{i1}^2 I_1(-w)} \quad , \tag{134}$$

where the speed ratio, w, is given by

$$w = \alpha_{i1} \bar{u}_{i1} \tag{135}$$

and the integrals I_k are defined by

$$I_k(b) = \int_b^\infty (\xi - b)^k \exp(-\xi^2) d\xi \quad . \tag{136}$$

The first few I_k are directly evaluated to give:

$$I_1(b) = \frac{1}{2}[\exp(-b^2) - b\sqrt{\pi}\ \mathrm{erfc}(b)] \quad , \tag{137}$$

$$I_2(b) = \frac{1}{4}[-2b \exp(-b^2) + (1 + 2b^2)\sqrt{\pi}\ \mathrm{erfc}(b)] \tag{138}$$

and

$$I_3(b) = \frac{1}{4}[2(1+b^2)\exp(-b^2) - b(2b^2+3)\sqrt{\pi}\,\mathrm{erfc}(b)] \quad . \tag{139}$$

11.3.4 Inversion to Determine Equilibrium Parameters

Combining Equations (133) and (134), it is possible to get a relation that involves only the sampled variables and the speed ratio, viz:

$$r \equiv \langle u_{il}^2 \rangle / (\langle u_{il} \rangle)^2 = \frac{I_1(-w)I_3(-w)}{[I_2(-w)]^2} \quad . \tag{140}$$

Since r, the ratio of the mean square velocity to the square of the mean velocity for molecules fluxing across the rectangular segment, is a function only of w, it is a useful place to start the inversion. As can be seen from Figure 4, r is monotonically decreasing with increasing w, going from an asymptote of 1.5 for $w \rightarrow -\infty$ to an asymptote of 1.0 for $w \rightarrow +\infty$. Since the function is monotonic, it can be inverted unambiguously as long as r falls within the interval ($1.0 < r < 1.5$). Although the functional form of r(w) is somewhat complex, making an analytic inversion impossible, a Newton-Raphson iteration starting at the center of the curve converges rapidly. Since this calculation is only done once for each segment to determine the boundary condition parameters, the time required for this inversion is negligible.

Once w is determined, then Equation (133) can be used to determine the corresponding value of α_{il}, which defines T_{il} via Equation (128). w and α_{il} determine $\overline{u}_{il}$ via Equation (135), and Equation (132) then determines n_i.

11.3.5 Possible Errors

In some cases, the procedure described above will not work directly, since the sampled value of r may exceed 1.5. This can be demonstrated by considering the simple case of two molecules, with velocities u_1 and u_2. The value of r sampled in this case approaches 2.0 as either molecule's velocity becomes much larger than the other. Hence, it is distinctly possible that values of r in excess of 1.5 will be encountered, either through statistical error or the failure of the assumption of an equilibrium type velocity distribution. (It is mathematically impossible to get a value of r less than 1.0, though numerical error might conceivable cause it in extreme cases.)

To handle these cases, as well as deal with some numerical problems that occur for large negative w, the inversion described in the previous section is performed only if the resulting value of w is within the range ($-5 < w < +5$). If r is such that w would fall outside of that range, w is set equal to ± 5 (depending on whether r is too large or too small), and the inversion procedure

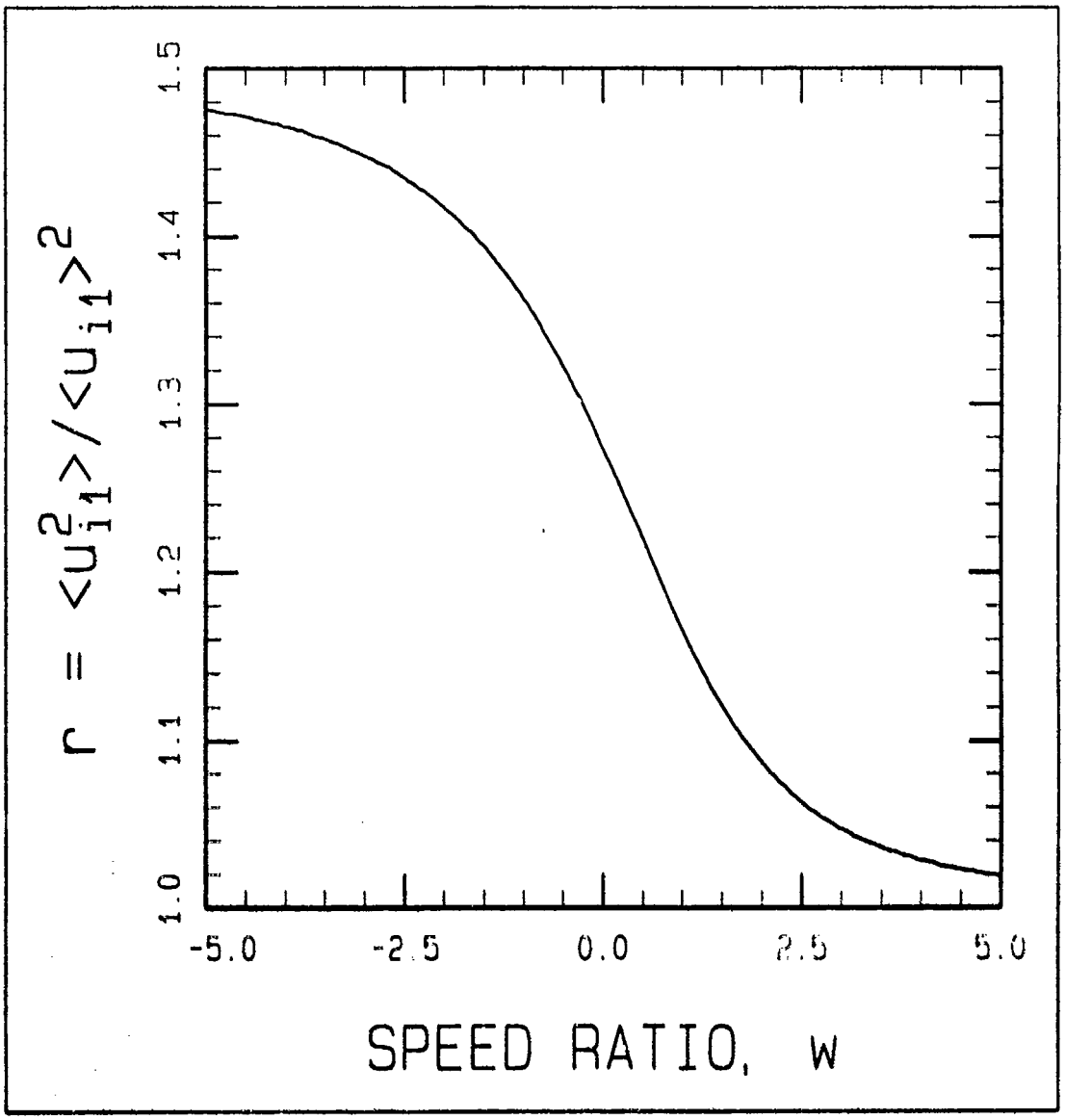

Figure 4. **A Graphical Representation of the Variable r, The Ratio of the Mean Square Velocity to the Square of the Mean Velocity for Molecules from a Maxwellian Velocity Distribution Fluxing Across a Plane, as a Function of the Speed Ratio, w.**

described above is then otherwise followed. The effect of this is that the derived boundary condition will match the statistically observed flux and mean velocity, but will no longer match the mean square velocity.

11.4 Spatial Variations

The rectangular element described in Subsection 11.3.2 will typically be a cell boundary in the outer solution. When the boundary condition is applied in the inner solution, it may comprise the boundary of several cells, since the inner solution will by definition have a finer cell mesh than the outer solution. It would be possible, of course, to merely apply the same boundary condition to each of the corresponding inner solution region cells, but with a little additional work it is possible to include some realistic spatial variation in the rectangular region, which may be used to provide adjacent inner region cells with slightly different boundary conditions. The procedure to do this is described in this section. This procedure allows for a spatial variation in flux (and therefore effective number density) along the rectangular region, but the velocity distribution is assumed to be spatially constant.

11.4.1 Reduction to Scaled Variables

Let the rectangle of interest be represented by the general variables $\hat{X}$ and $\hat{Y}$, such that $(\hat{X}_1 < \hat{X} < \hat{X}_2)$ and $(\hat{Y}_1 < \hat{Y} < \hat{Y}_2)$. Then it is convenient to introduce the scaled variables, X and Y, such that

$$X = -1 + 2\frac{\hat{X} - \hat{X}_1}{\hat{X}_2 - \hat{X}_1} \tag{141}$$

and

$$Y = -1 + 2\frac{\hat{Y} - \hat{Y}_1}{\hat{Y}_2 - \hat{Y}_1} \quad . \tag{142}$$

The scaled variables have the advantage that they each traverse the range of -1 to +1.

11.4.2 Spatial Moments

As molecules traverse the rectangular region in question, it is possible to calculate the X and Y values at which a given molecule crosses it. Sums of these values can also be kept, so that a statistical determination can be made of the average X value, $<X>$, the average Y value, $<Y>$, and the average product of the two, $<XY>$. At the same time, of course, the average flux across the rectangle will also be determined.

11.4.3 Analytic Representation of Sampled Moments

Let j(X,Y) be flux distribution in the rectangular region (molecules per unit area per unit time). The number of molecules crossing the rectangle per unit time, $\dot{N}$, is therefore given by:

$$\dot{N} = \int_{-1}^{1}\int_{-1}^{1} j(X,Y)\, dXdY \quad . \tag{143}$$

The average sampled values given in the previous section can therefore be represented via

$$\langle X \rangle = \frac{1}{\dot{N}} \int_{-1}^{1}\int_{-1}^{1} j(X,Y)\, XdXdY \quad , \tag{144}$$

$$\langle Y \rangle = \frac{1}{\dot{N}} \int_{-1}^{1}\int_{-1}^{1} j(X,Y)\, YdXdY \tag{145}$$

and

$$\langle XY \rangle = \frac{1}{\dot{N}} \int_{-1}^{1}\int_{-1}^{1} j(X,Y)\, XYdXdY \quad . \tag{146}$$

11.4.4 Assumed Form for the Flux Distribution

It is assumed that the flux distribution can be adequately represented by a linear distribution, viz.

$$j(X,Y) = \dot{N}(a_0 + a_1X + a_2Y + a_3XY) \quad . \tag{147}$$

When this form is substituted into the integrals defined in Equations (143) - (146), there results:

$$a_0 = \frac{1}{4} \quad , \tag{148}$$

$$a_1 = \frac{3\langle X \rangle}{4} \quad , \tag{149}$$

$$a_2 = \frac{3\langle Y \rangle}{4} \tag{150}$$

and

$$a_3 = \frac{9\langle XY \rangle}{4} \quad . \tag{151}$$

Hence, under the assumption of a linear flux distribution, the spatial moments lead immediately to the corresponding linear coefficients.

11.4.5 Possible Problems

Since the flux that is discussed above is the one-way flux (i.e., only counting molecules traveling in one direction across the rectangular segment), it is by definition a quantity which can never be negative. However, again due to either statistical error or the invalidity of the assumed functional form, it is conceivable that the distribution derived above could become negative at some subregion of the rectangle. If this does occur, corrections must be made to the coefficients.

In order to search for a negative subregion, it suffices to investigate the corner values, since the maximum and minimum must occur on the corners for a linear fit. The corner values are given directly by

$$j_{11} = j(-1,-1) = \dot{N}(a_0 - a_1 - a_2 + a_3) \quad , \tag{152}$$

$$j_{12} = j(-1,+1) = \dot{N}(a_0 - a_1 + a_2 - a_3) \quad , \tag{153}$$

$$j_{21} = j(+1,-1) = \dot{N}(a_0 + a_1 - a_2 - a_3) \tag{154}$$

and

$$j_{22} = j(+1,+1) = \dot{N}(a_0 + a_1 + a_2 + a_3) \quad . \tag{155}$$

If a negative value is found, then use can be made of the inverse relations, which give the a_i as a function of the corner values, i.e.,

$$a_0 = \frac{1}{4N}(+j_{11} + j_{12} + j_{21} + j_{22}) \quad , \tag{156}$$

$$a_1 = \frac{1}{4N}(-j_{11} - j_{12} + j_{21} + j_{22}) \quad , \tag{157}$$

$$a_2 = \frac{1}{4N}(-j_{11} + j_{12} - j_{21} + j_{22}) \tag{158}$$

and

$$a_3 = \frac{1}{4N}(+j_{11} - j_{12} - j_{21} + j_{22}) \quad . \tag{159}$$

If one of the corner values is negative, then it can be artificially increased to zero, while one third the amount added to the negative corner is subtracted from each of the other corner values. This procedure keeps a_0, and therefore the integrated total flux, constant. Once the corner values have been adjusted so that none are negative, Equations (156) - (159) give the corresponding linear coefficients.

12. COMPARISON OF SHUTTLE ENGINE FIRINGS IN SPACE TO CODE PREDICTIONS

12.1 Introduction

This section describes a model/data comparison for some visible data taken by the Air Force Maui Optical Station (AMOS) of 870 lb. shuttle RCS firings at altitudes around 320 km. The data are unique in that they were obtained for three angles of attack: 0°, 90°, and 180°. The sequence of events was to fire in one direction for three seconds and then shut down for five seconds before firing another engine in another direction. The data which are being utilized in this paper involve total visible plume intensity as measured by an S-20 photocathode, and its spectral dependence as measured by a spectrograph. In particular, we are concentrating on a peak in the spectrum at 6300 Å which is being attributed to the forbidden transition between the $O(^1D)$ excited electronic state and the $O(^3P)$ ground state. This emission is intriguing because the long ($\approx$ 194 seconds[9]) radiative lifetime of the excited state would normally be associated with a very weak, spatially diffuse signature. However, the quenching of the $O(^1D)$ state is sufficiently rapid at this altitude that the net lifetime of the excited state is more in the vicinity of one second, providing a much less diffuse signature than would exist in the absence of quenching. Furthermore, the abundance of atomic oxygen is sufficient to produce a measurable signature even at this reduced lifetime.

The existence of a single set of well characterized unsteady data as a function of angle of attack provides an excellent opportunity to do model comparisons with the hope of discerning the underlying mechanism(s). Two mechanisms were hypothesized as potentially being responsible for this emission: the charge exchange reaction between atmospheric O^+ ions and H_2O from the exhaust, and the direct collisional excitation of the $O(^1D)$ state. These data provide a stressing validation case for the SOCRATES code, as well as an opportunity to learn about a new visible plume emission source.

12.2 Experiment

The experiment consisted of firing specific 870 lb. PRCS liquid-fuel (monomethyl hydrazine-N_2O_4) engines while the shuttle orbiter passed over AMOS atop Mt. Haleakala, Maui, HI (21°N, 204°E, 3000 m altitude). The engines were fired for angles of attack of 180°, 90°, and 0° with respect to the ambient, which will be referred to as ram, perpendicular, and wake burns, respectively. The shuttle was in total darkness (the solar and lunar depression angles at the shuttle were 30° and 59°, respectively). Imagery data were obtained using 8" and 22" acquisition telescopes. Visible spectral data were obtained using a spectrograph with its own foreoptics mounted on the main telescope. The spectral, spatial, and temporal properties of the emissions were measured as a function of angle of attack of the exhaust products by the atmosphere. The total plume intensity for an S-20 photocathode was estimated using the 6° GEODSS telescope which had a fixed field of view. This field of view was sufficient to encompass the entire plume, and its

fixed nature enabled known stars to be used for calibration. The experiment is described in more detail in Reference 10.

12.3 Data Reduction

On the basis of comparing against a known star in the GEODSS field of view, the peak total plume emission for an S-20 photocathode was estimated to be 150, 80, and 12 W/sr for the ram, perpendicular, and wake burns, respectively. An average spectrum shows a substantial NH peak around 3360 Å, a peak around 6800 Å due to second order diffraction of the NH(A→X) fundamental, as well as several other peaks. For the present purposes, the quantity of interest is the total emission from the 6300 Å atomic oxygen line. To estimate this, the spectrum was multiplied by an S-20 response curve and integrated over the spectral range. The ratio of the integral between 6100 and 6500 Å to the total integral was estimated to be the fraction of the total S-20 response which was due to the 6300 Å transition. For the present case this ratio came out to be 12%. It should be noted that a more proper approach would be to do the same averaging for spectra resulting from burns in the three directions, since the varying available kinetic energy may shift the relative magnitudes of the emission peaks as a function of angle of attack.

The atomic oxygen Green line ($O(^1S)\rightarrow O(^1D)$) at 5577 Å is not observed in any of the burns. Based on the increased activation energy required for excitation of the $O(^1S)$ state this seems reasonable. The $O(^1S)$ lies at 4.2 eV above the $O(^3P)$ ground state as compared to 2.0 eV for the $O(^1D)$ state. For the 0 and 90 degree burns the maximum available collisional energy is not sufficient to reach the $O(^1S)$ level. At 180 degrees there is enough collisional energy to excite the Green line emission, but it is still expected to be less than the Red line signal. The issue of the relative Green line intensity for the retro-fire case is planned for a future investigation.

12.4 Modeling Approach

The atmospheric and exhaust mole fractions of the species considered in the calculations are given in Table 2. The modeling efforts focused on simulating the overall character of the plumes in the three orientations, and in trying to understand the 6300 Å data feature, which is being attributed to the forbidden transition between the $O(^1D)$ excited state and the $O(^3P)$ ground state. Since the $O(^1D)$ state has a long radiative lifetime, it was expected that quenching would be an essential element of the calculations. The following rate constants (in cm^3/s) from the literature were used:

$$O(^1D) + N_2 \rightarrow O + N_2 \qquad k^{11} = 2.3\times10^{-11} \tag{160}$$

$$O(^1D) + O \rightarrow O + O \qquad k^{12} = 8.8\times10^{-12} \tag{161}$$

$$O(^1D) + H_2O \rightarrow 2OH \qquad k^{13} = 2.2\times10^{-10} \tag{162}$$

Table 2. Concentrations of Species Carried in the Model Calculations.

Species	Atmospheric Mole Fraction	Exhaust Mole Fraction
O	0.9076	0.0
N_2	0.0919	0.309
H_2	0.0	0.187
H_2O	0.0	0.332
CO	0.0	0.136
CO_2	0.0	0.036
O^+	0.0005	0.0

Published rate constants or cross sections for the collisional excitation of the $O(^1D)$ state could not be found, so microscopic reversibility was invoked to estimate the following excitation rate constants:

$$O + N_2 \rightarrow O(^1D) + N_2 \qquad k = 1.28\times10^{-11}\exp(-\frac{22800}{T}) \tag{163}$$

$$O + O \rightarrow O(^1D) + O \qquad k = 4.9\times10^{-12}\exp(-\frac{22800}{T}) \tag{164}$$

Reaction (163) was also assumed to apply for the other major plume constituent, H_2O. The charge exchange mechanism for producing $O(^1D)$ was represented by

$$O^+ + H_2O \rightarrow O(^1D) + H_2O^+ \qquad k = 3.23\times10^{-9}T^{-0.34}\exp(-\frac{11600}{T}) \quad . \tag{165}$$

The rate constant for Reaction (165) was taken from measured values[14] with the activation energy adjusted to reflect the additional energy required to create the $O(^1D)$ rather than the $O(^3P)$ product.

12.5 Results And Conclusions

Grayscale plots are given in Figures 5-7 showing the calculated evolution of the 6300 Å ram plume radiance as a function of time. There is a substantial qualitative resemblance to the data in these plots, though a quantitative comparison of these images is difficult. Recall that the engine shuts off at 3.0 seconds, so the spreading and reducing of the signature at 4.0 seconds in Figure 7 is to be expected. The total calculated 6300 Å radiant intensity as a function of time is given in Figure 8 for the three angles of attack. If the peak values from this figure are compared to the deduced data values, then the result is the comparison shown in Figure 9. The agreement in Figure 9 is probably fortuitously good, since it is doubtful that even the input quantities were known that

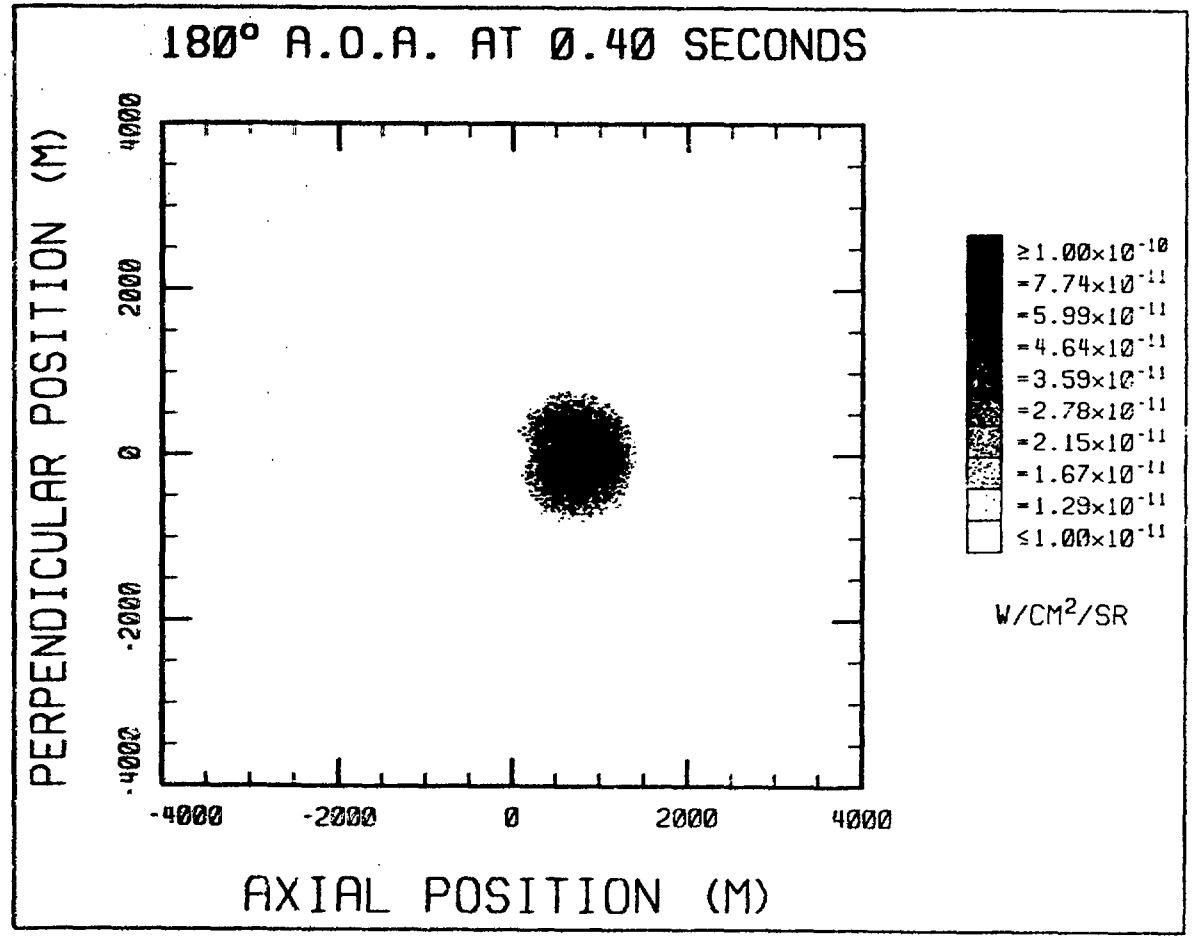

Figure 5. **A Grayscale Plot Showing the Calculated 6300 Å Plume Radiance for a Ram Burn at 0.4 Seconds. The Shuttle is Located at the Center of the Plot, and the Wind is Approaching from the Right.**

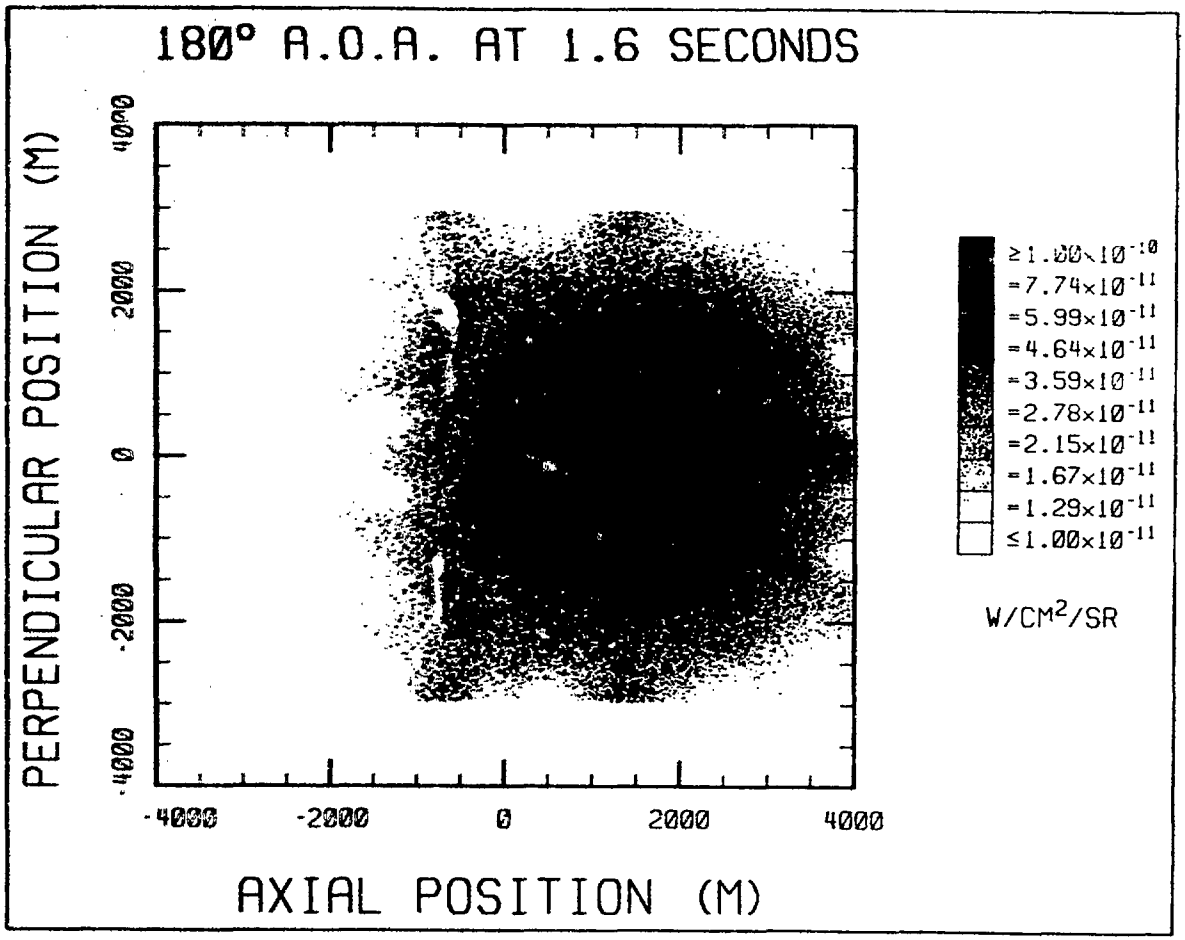

Figure 6. **A Grayscale Plot Showing the Calculated 6300 Å Plume Radiance for a Ram Burn at 1.6 Seconds. The Shuttle is Located at the Center of the Plot, and the Wind is Approaching from the Right.**

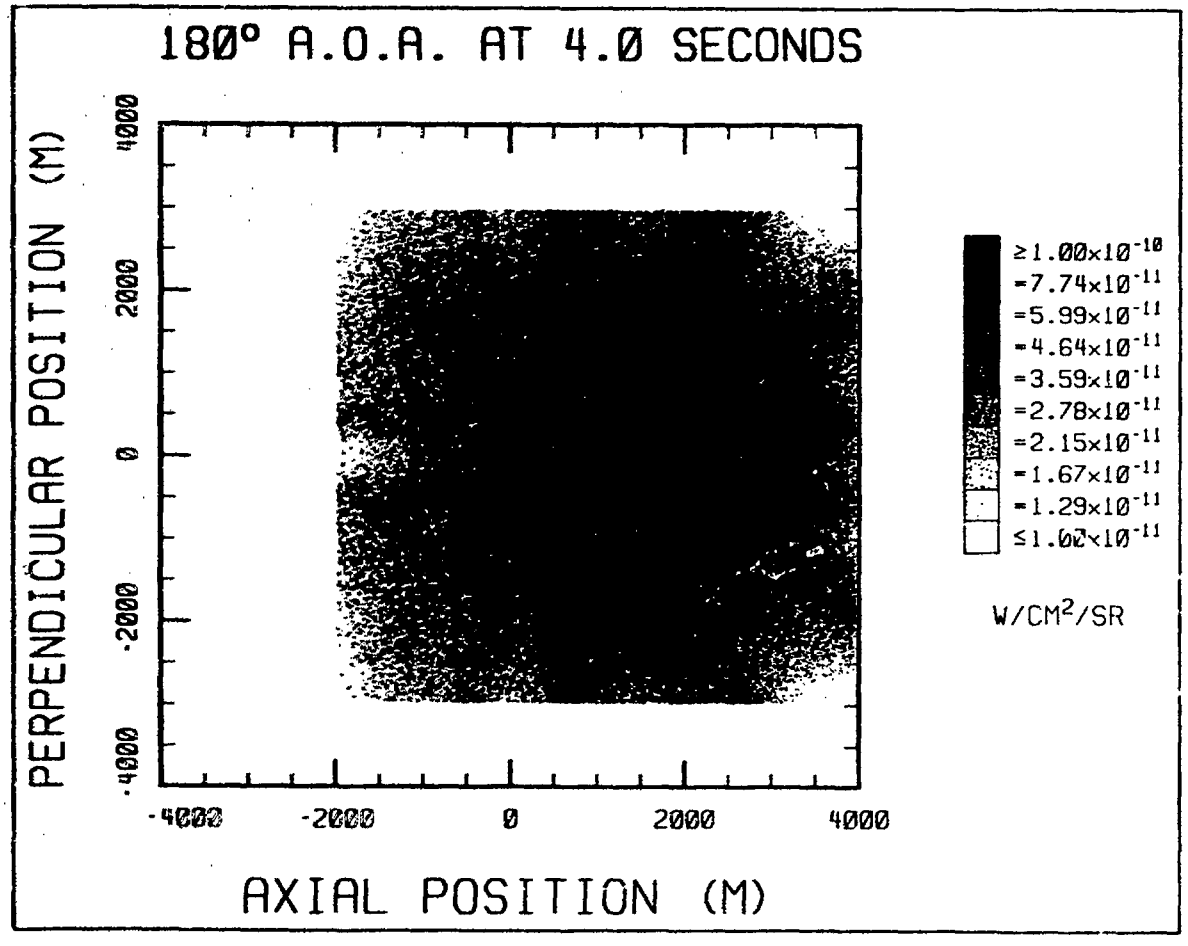

Figure 7. **A Grayscale Plot Showing the Calculated 6300 Å Plume Radiance for a Ram Burn at 4.0 Seconds. The Shuttle is Located at the Center of the Plot, and the Wind is Approaching from the Right.**

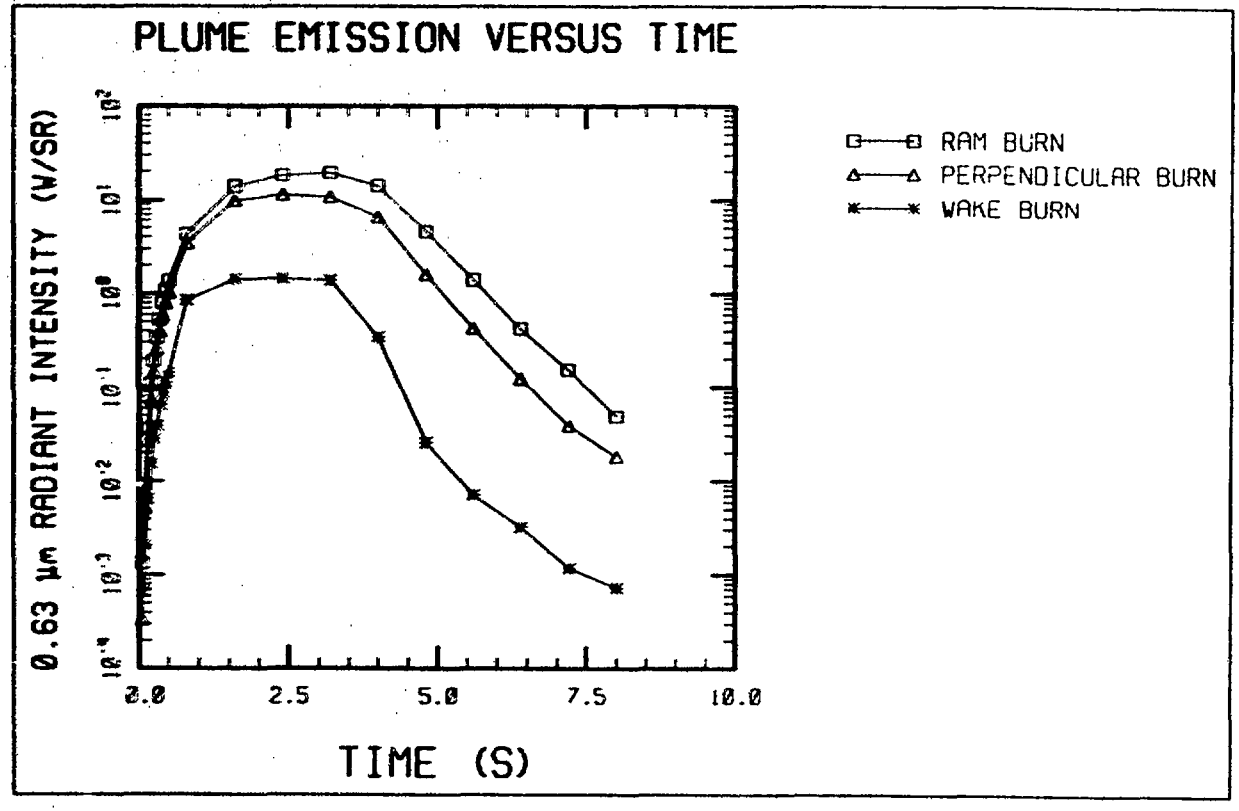

Figure 8. **The Calculated Total 6300 Å Radiant Intensity as a Function of Time for the Three Burn Directions.**

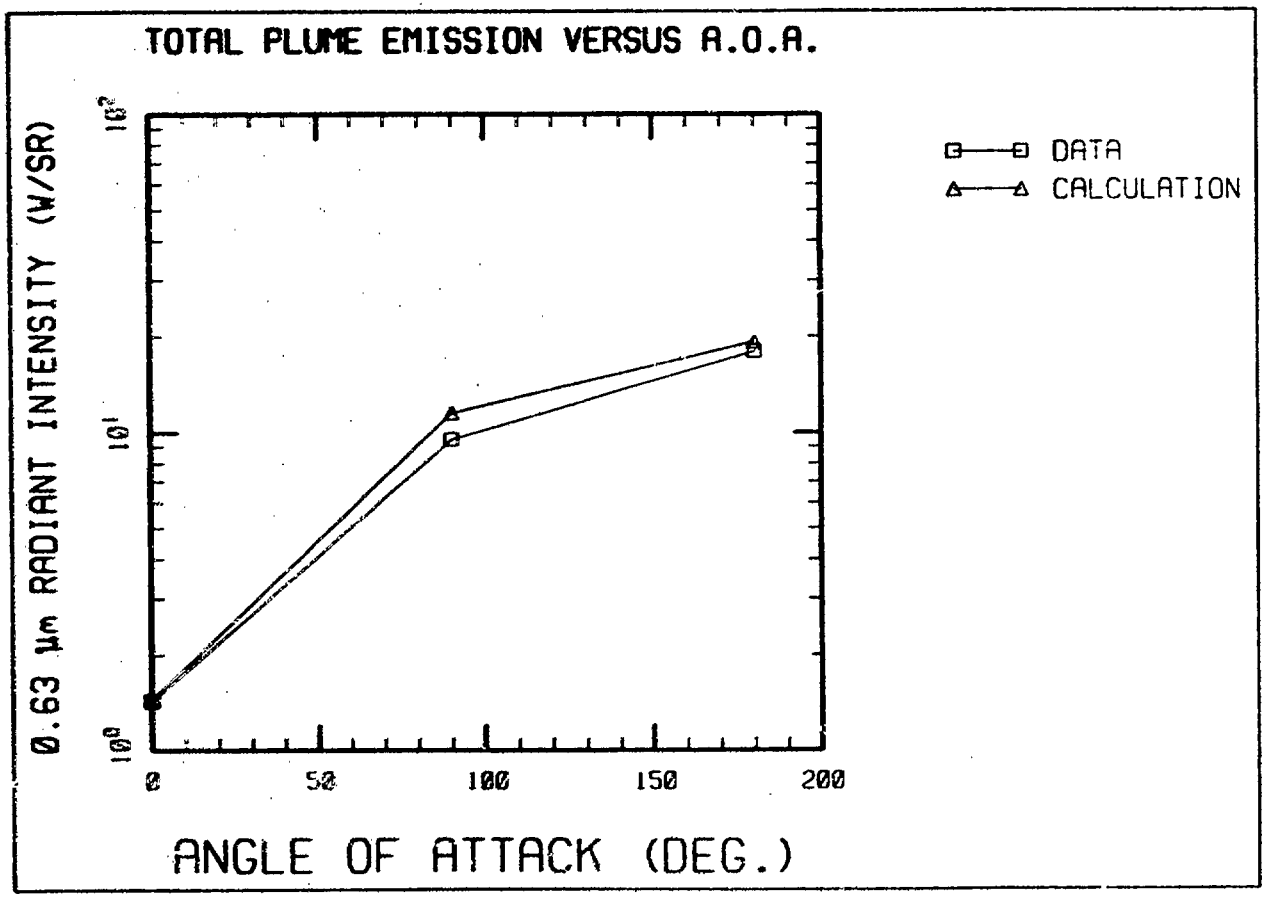

Figure 9. **A Comparison Between the Calculated and Deduced Peak Total 6300 Å Plume Emission as a Function of Angle of Attack.**

accurately. Nevertheless, the agreement is impressive and strongly supportive of the hypothesized mechanisms.

Given confidence in the basic description, it is then possible to use the model to get more quantitative and qualitative understanding of the underlying physics. The major difference to be expected in the excitation mechanisms is the activation energy required; the charge exchange mechanism requires a lower activation energy and, therefore, would be expected to be relatively more important for lower angles of attack. This is illustrated in Figures 10-12, where the integrated excitation rate of the $O(^1D)$ state is shown as a function of time for 180°, 90° and 0° angles of attack respectively. The separate contributions are shown for the two mechanisms in the figures, and it can be seen that the charge exchange mechanism is calculated to contribute 3.2% as much as the collisional excitation mechanism at 180°, 3.9% at 90°, and 12.7% at 0°. (These comparisons are made at the end of the burn.) Hence, the general trend of increasing importance of charge exchange with decreasing angle of attack is confirmed, though it should be noted that the charge exchange rate is never calculated to be a large fraction of the total signature, so it can not be confidently deduced that that portion of the calculation is being carried out properly.

Given the lower activation energy requirement of the charge exchange mechanism, it might also be supposed that it would gain in importance for the shutdown transient as the flow energy decreases. As can be seen in particular for 0° in Figure 12, the exact opposite is true - the relative importance of the charge exchange mechanism drops by over four orders of magnitude after shutdown. The reason for this precipitous drop is shown in Figure 13, which shows the total number of water molecules in the solution region as a function of time. The number of water molecules understandably drops by several orders of magnitude since the wind and the exhaust direction are coaligned. Within a second it is to be expected that the vast majority of the water molecules, initially traveling at 3.5 km/s and generally accelerated by the free stream, will tend to leave the solution region which only extends four kilometers downstream of the exit.

The question remains, however, as to the origin of the collisional excitation after the plume has largely departed the solution region. The explanation for this is given in Figure 14, which shows the contributions of the various types of collisions to the total collisional excitation rate. While the thruster is on, most of the excitation comes from $O\text{-}N_2$ collisions. This is to be expected, since the rate constant for Reaction (1) is quite high, and N_2 is a major plume species with a fairly large molecular weight (and therefore relative collision energy). However, after shutdown the curves cross, and O-O collisions become the dominant source of excitations. The $O\text{-}H_2O$ collisions do drop in importance as the plume leaves the solution region, but the $O\text{-}N_2$ collisions do not drop nearly as much. This is because N_2 is also present in the atmosphere, so it is not leaving the solution region in the same way that the H_2O is. The conclusion is that the shutdown transient is dominated by continued collisions within the atmosphere that remains disturbed for a while after the engine shuts down. It is a fundamental difference attributable to looking at radiation from an atmospheric rather than a plume species, and it would have been difficult to guess this effect without a comprehensive model calculation. The same switch of important collision class can be seen in Figure 15 for the 180° case, but the magnitude of the effect

is not as important here. The reason is that for a retrofire case the plume molecules remain in the solution region longer since they are initially heading into the free stream and then get turned around and travel backwards relative to their initial motion. The increased residence time of plume species within the solution region allows atmosphere-plume collisions to retain their importance for a longer period of time after shutdown.

The question of excited state lifetime is addressed in Figure 16. This figure shows the overall contributions of collisional quenching and radiative decay to the disappearance of the $O(^1D)$ state as a function of time for the 180° case. While the engine is in operation, an $O(^1D)$ atom is about ten times as likely to suffer collisional quenching as to experience radiative decay. Hence, the effective excited state lifetime is about twenty seconds while the engine is operating, on the average. If just the brightest portion of the plume is inspected (where the collision and quenching rates are particularly high) the deduced species lifetime is more like 1-2 seconds. The conclusion is that the actual species lifetime will depend greatly on where in the plume the species is produced. After shutdown, the two overall depletion mechanisms become comparable, and the $O(^1D)$ is predicted to have a lifetime on the order of 100 seconds. Again, this number would be expected to vary depending on how collisional the region in which it is formed is.

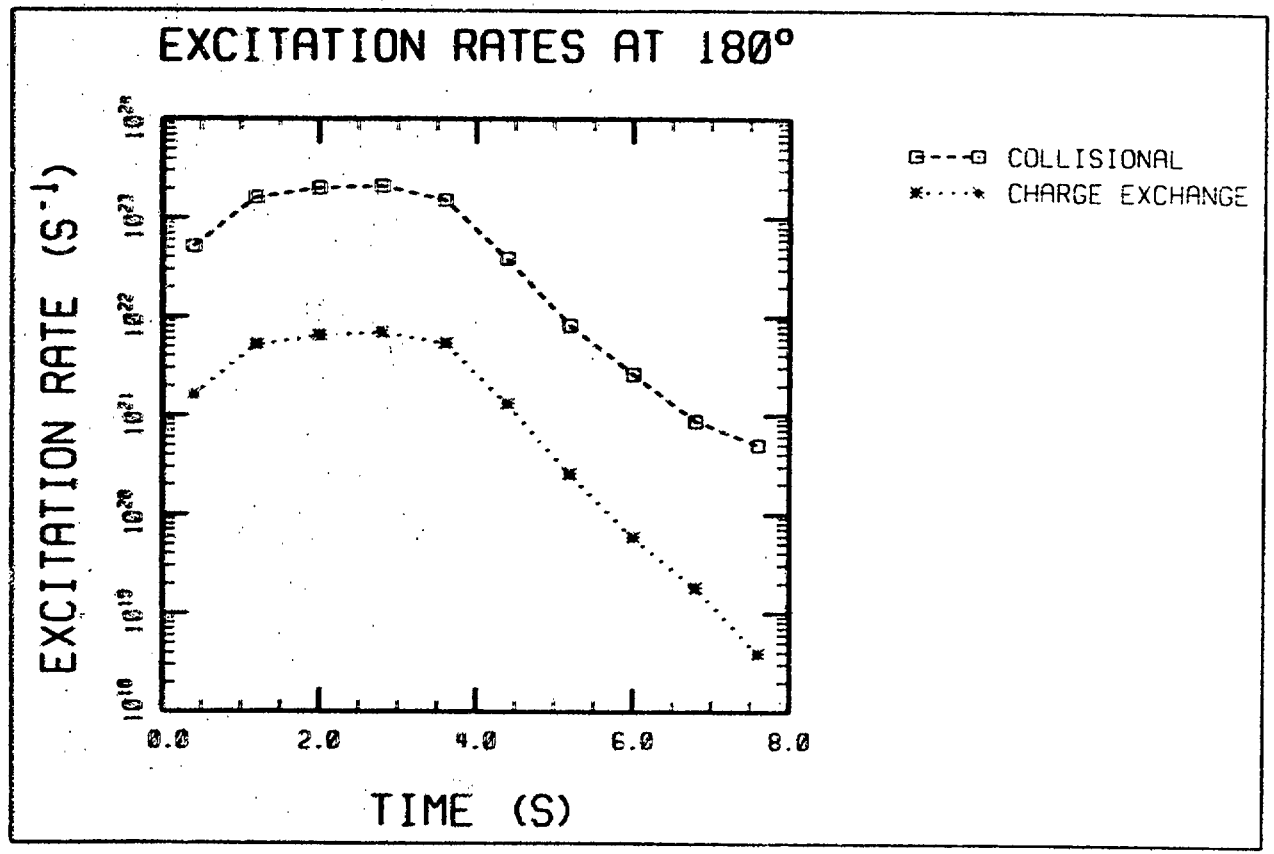

Figure 10. **The Calculated Contributions of Collisional Excitation and Charge Exchange to O(¹D) Production as a Function of Time for the 180° Angle of Attack Case.**

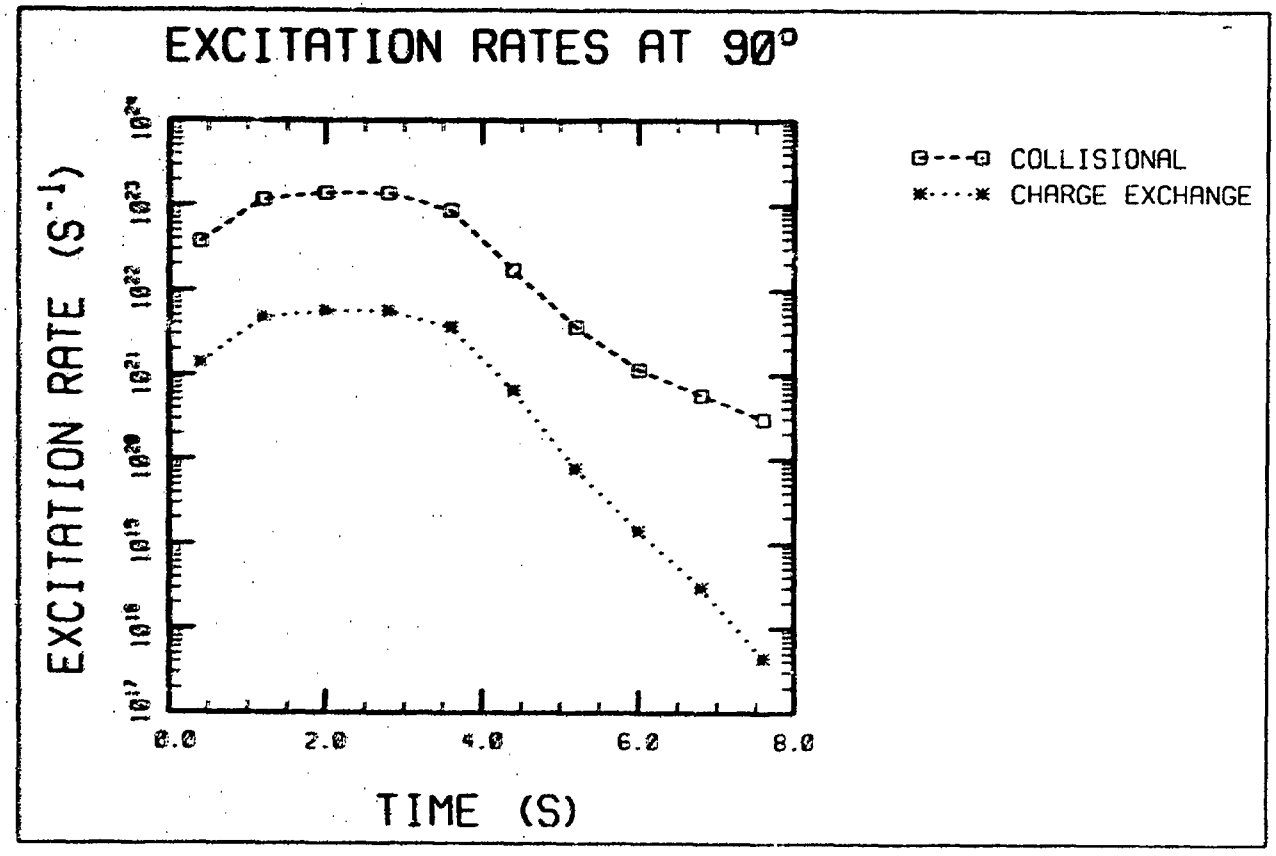

Figure 11. **The Calculated Contributions of Collisional Excitation and Charge Exchange to O(¹D) Production as a Function of Time for the 90° Angle of Attack Case.**

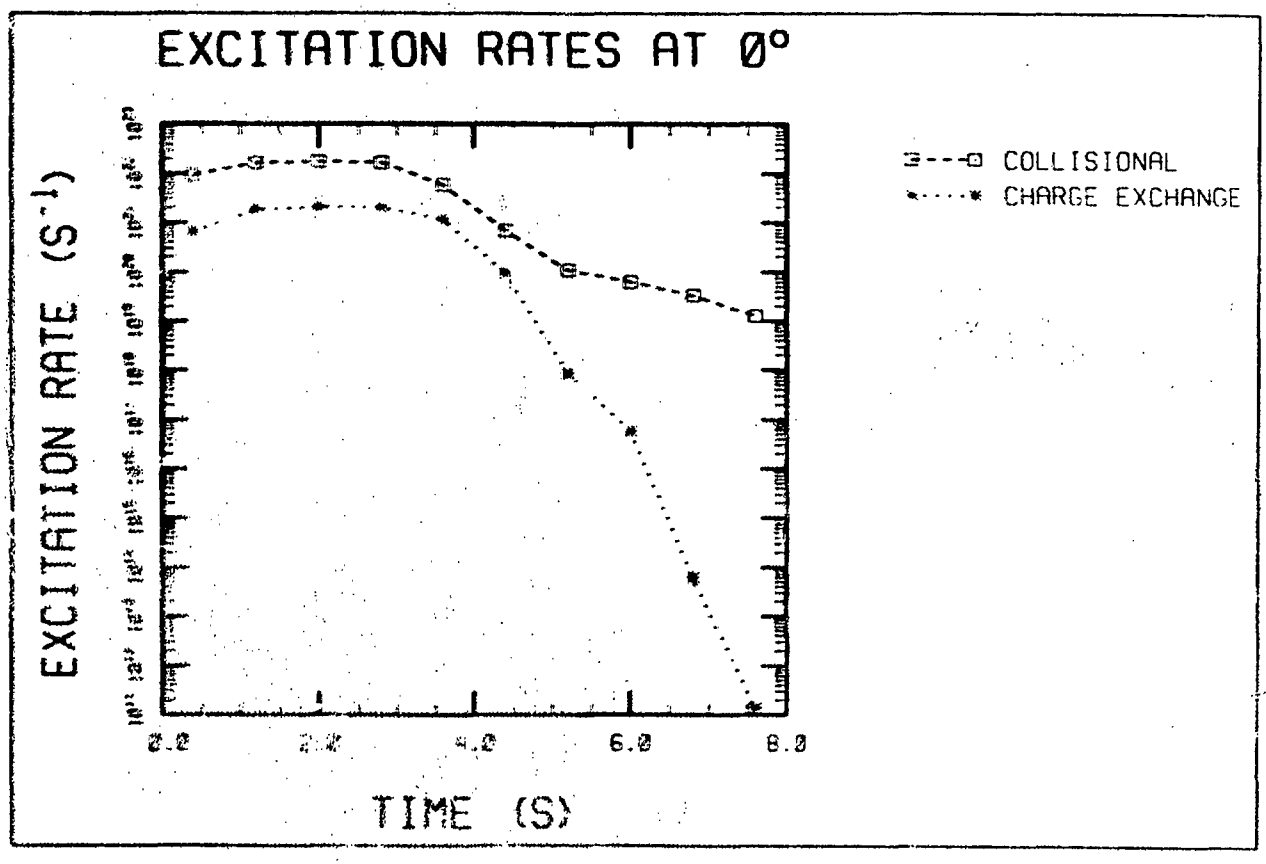

Figure 12. The Calculated Contributions of Collisional Excitation and Charge Exchange to O('D) Production as a Function of Time for the 0° Angle of Attack Case.

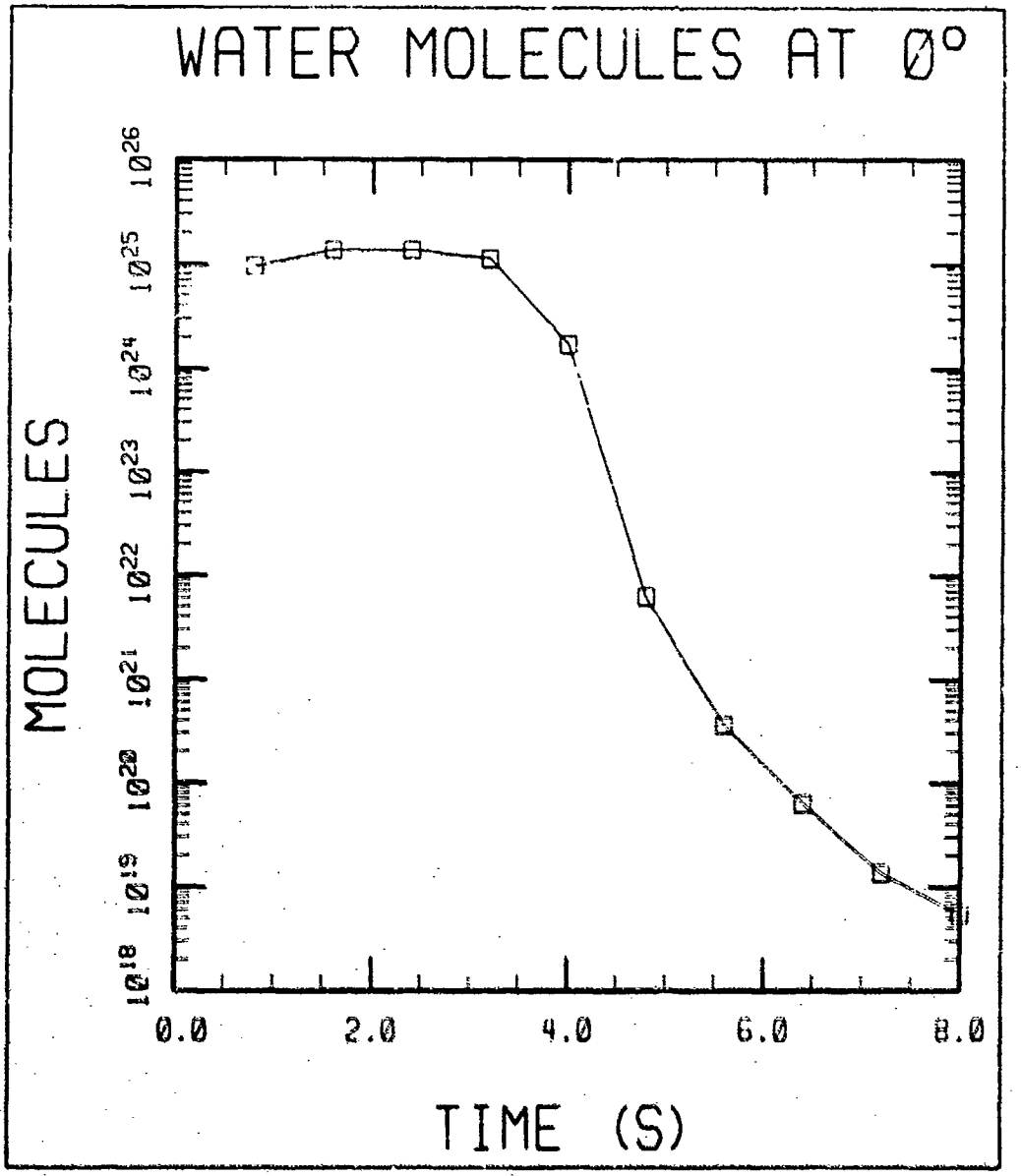

Figure 13. **The Total Number of Water Molecules in the 0° Solution Region as a Function of Time.**

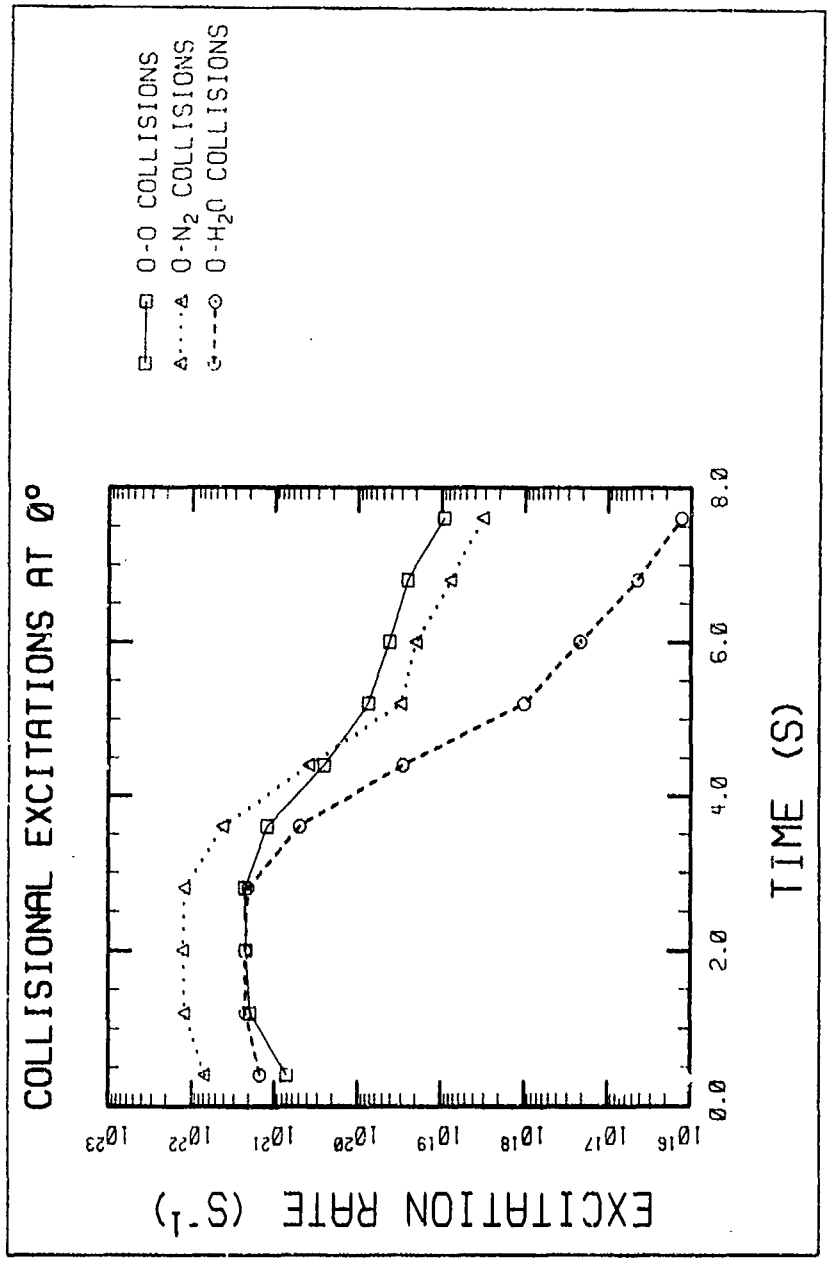

Figure 14. The Contributions of the Three Types of Excitation Collisions Considered as a Function of Time for the 0° Angle of Attack Case.

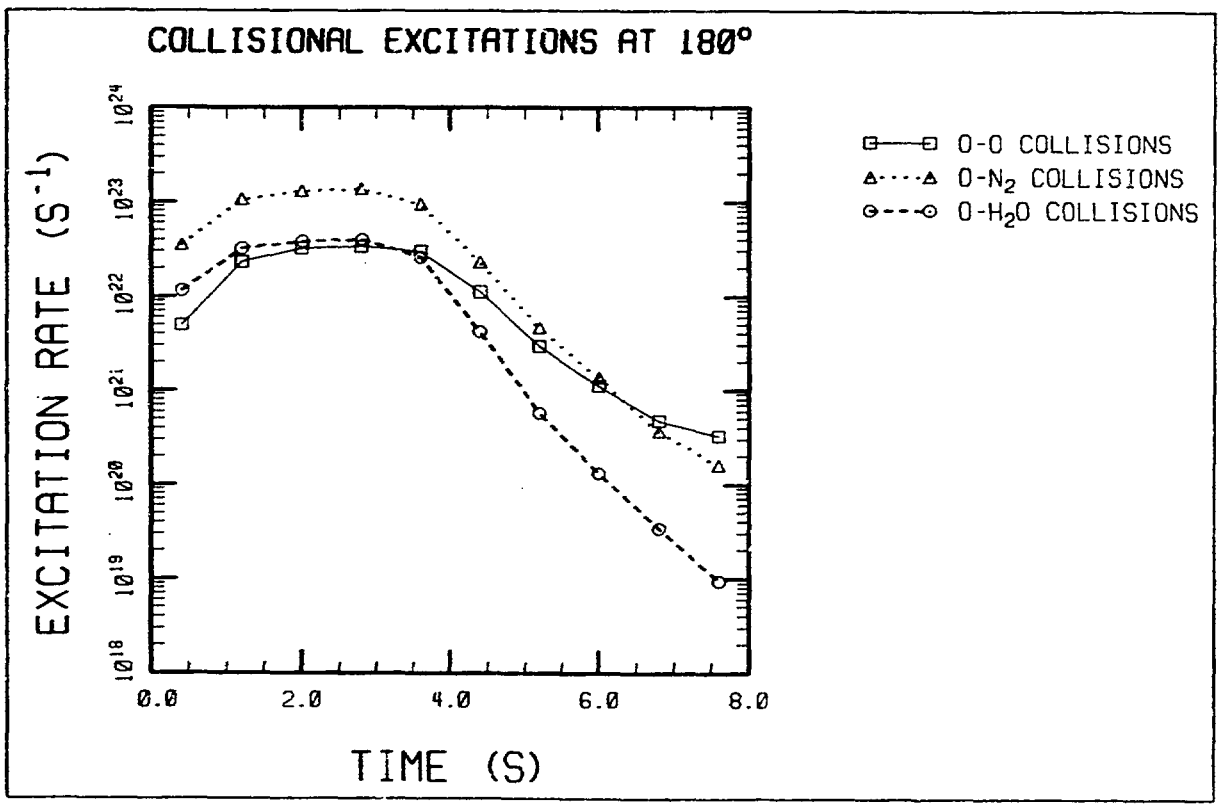

Figure 15. The Contributions of the Three Types of Excitation Collisions Considered as a Function of Time for the 180° Angle of Attack Case.

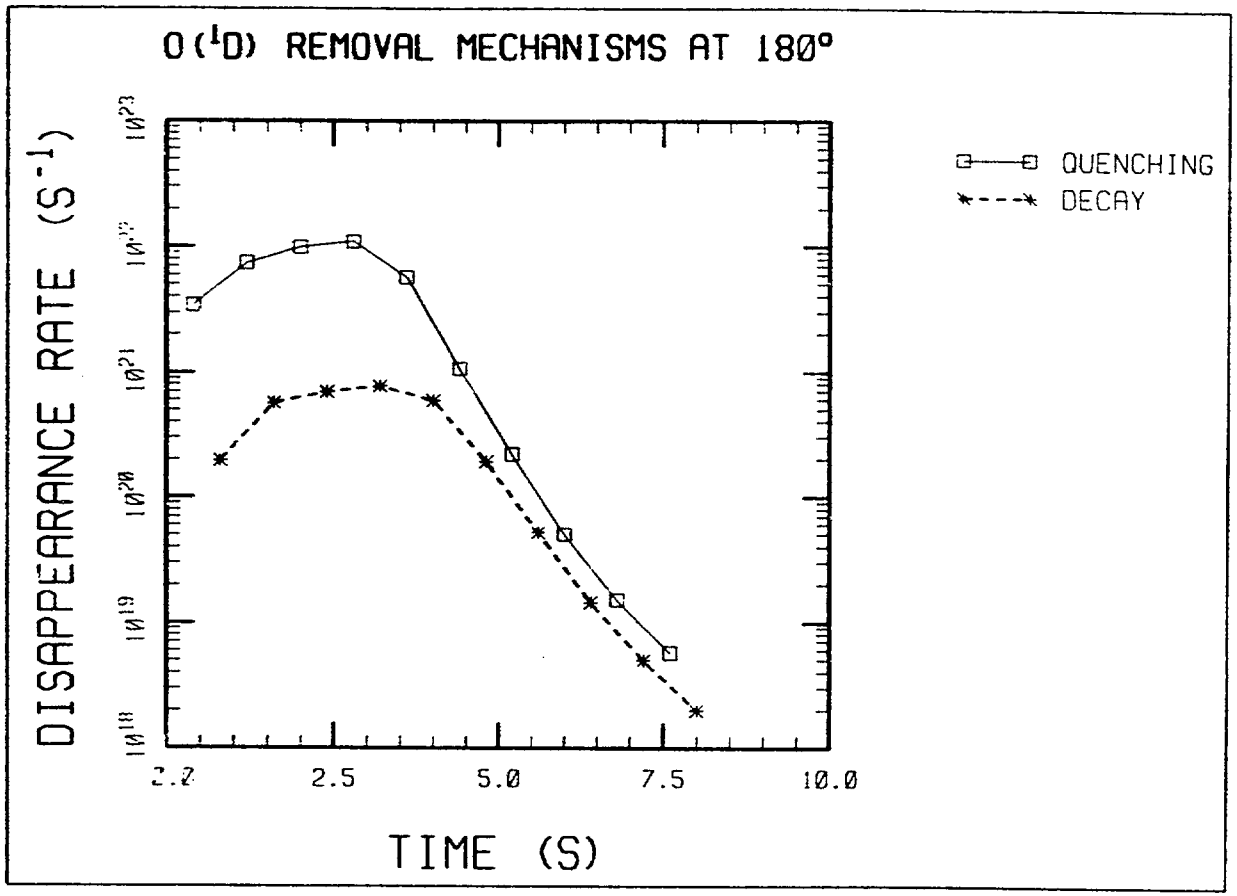

Figure 16. The Competing Effects of Collisional Quenching and Radiative Decay as a Function of Time for the 180° Angle of Attack Case.

13. SUMMARY

The present version of the SOCRATES code should be regarded as the latest step in an ongoing development project. Particular emphasis has been paid to making it easy for a non-expert to use, while sacrificing neither rigor nor flexibility. Future versions are expected to allow for a gas dynamic interaction with the solid bodies as well multiple source types. Even without these features, the present model is a powerful tool which can be used for data analysis and first principles predictions.

The sample calculations present some important insight into visible emission from plumes in the 6300 Å region. They indicate that collisional excitation of the electronic state is the dominant mechanism explaining the observed emission. This emission is particularly significant since it arises from the atmosphere itself, so it is therefore largely independent of fuel type.

14. REFERENCES

1. G. A. Bird, *Molecular Gas Dynamics*, Clarendon Press, Oxford (1976).

2. S. Chapman and T. G. Cowling, *The Mathematical Theory of Non-Uniform Gases*, 3rd ed., Cambridge University Press, Cambridge, p. 86 (1970).

3. G. A. Bird, "Monte-Carlo Simulation in an Engineering Context," Proceedings of the 12th International Symposium on Rarefied Gas Dynamics, *Progress in Astronautics and Aeronautics*, 74, AIAA, New York (1981).

4. Borgnakke, Claus, and Larsen, P. S., "Statistical Collision Model for Monte Carlo Simulation of Polyatomic Gas Mixture", *Journal of Computational Physics*, 18, 405 (1975).

5. J. B. Elgin and R. L. Sundberg, "Model Description for the SOCRATES Contamination Code," Report AFGL-TR-88-0303, Air Force Geophysics Laboratory, Hanscom AFB, MA (1988) ADA205818.

6. J. W. Brook, "Far Field Approximation for a Nozzle Exhausting into a Vacuum," *Journal of Spacecraft and Rockets*, 6, 626 (1969).

7. J. B. Elgin, "Getting the Good Bounce: Techniques for Efficient Monte Carlo Analysis of Complex Reacting Flows," Report SSI-TR-28, Spectral Sciences, Inc., Burlington MA (1983).

8. W. G. Vincenti and C. H. Kruger, Jr., *Introduction to Physical Gas Dynamics*, John Wiley and Sons, p. 348 (1965)

9. J. H. Kernahan and P. H. L. Pang, "Experimental Determination of Absolute A Coefficients for 'forbidden' Atomic Oxygen Lines," *Canadian Journal of Physics*, 53, 455 (1975).

10. E. Murad, D. J. Knecht, R. A. Viereck, C. P. Pike, I. L. Kofsky, C. A. Trowbridge, D. L. A. Rall, G. Ashley, L. Twist, J. B. Elgin, A. Setayesh, A. T. Stair, Jr., and J. E. Blaha, "Visible Light Emission Excited by Interaction of Space Shuttle Exhaust with the Atmosphere", *Geophysical Research Letters*, 17, 12, pp. 2205-2208 (Nov. 1990).

11. R. J. Link, J. C. McConnell, G. G. and Shepard, "A Self-consistent Evaluation of the Rate Constants for the Production of the O 6300 Å Airglow," *Planetary and Space Science*, 29, pp. 589-593 (1981).

12. Y. Sun, and A. Dalgarno, "Collisional Excitation of Metastable O(^{1}D) Atoms," *J. Chem. Phys.*, 96, 5017-5019 (1992).

13. K. H. Gericke and F. J. Comes, "Energy Partitioning in the Reaction O(^{1}D)+H_2O → 2OH. The Influence of O(^{1}D) Translational Energy on the Reaction Rate Constant," *Chem. Phys. Lett.*, 81, 218 (1981).

14. M. Heninger, S. Fenistein, G. Mauclaire, R., Marx, and E. Murad, "Review of the Reaction of O^+ with H_2O and its Bearing on Composition Measurements from the Space Shuttle," *Geophysical Research Letters*, 16, 2, pp. 139-141 (1989).